

Characteristics of tides in the Bay of Bengal

B. Sindhu* and A. S. Unnikrishnan

*CSIR National Institute of Oceanography
Dona Paula, Goa, 403004, India*

*Present affiliations: COWI Gulf A/S
Dubai, UAE, PO Box 52978*

Abstract

A vertically integrated 2D numerical model was developed for the simulation of major tidal constituents (M_2 , S_2 , N_2 , K_1 and O_1) in the Bay of Bengal. The bathymetry for the model domain was derived from an improved ETOPO5 dataset prepared in our earlier work. Composite tidal elevations and the amplitudes and phases of the respective tidal constituent extracted from the global tidal model FES2004 along the open boundary were used for the simulation of composite tides and tidal constituents, respectively. The simulated tidal elevations at Paradip, Visakhapatnam, and Chennai showed good agreement with the hourly tide gauge observations at these locations. The amplitudes and phases of M_2 , S_2 , K_1 and O_1 at the coastal stations, obtained from harmonic analysis of simulated tides, were found to agree well with those obtained from Admiralty Tide Tables with the RMS misfit 9.2, 5.6, 2.9 and 3.1 cm, respectively. In the Bay of Bengal, semi-diurnal tides (M_2 , S_2 , and N_2) attain highest amplitudes (180, 80, 30 cm, respectively) in the Gulf of Martaban while amplitudes of diurnal tides (K_1 , O_1) reaches maximum (20, 12 cm, respectively) in the Malacca Strait. Semidiurnal tides are found to amplify significantly in the head bay, along the southern coast of Myanmar and in the Gulf of Martaban with amplification factor (AF, the ratio of tidal amplitude at coastal station to that at the shelf break) of 1.9, 2.0, 2.4, respectively (M_2). The diurnal tides amplify significantly in the north eastern end of the head bay and in the Gulf of Martaban region with AF (for K_1) of 1.5, 1.7, respectively. The continental shelf in the head bay and along the southern coast of Myanmar is about 200 km wide and the amplitudes of semi-diurnal tides are doubled in these regions while the diurnal tides amplify only marginally, which is consistent with Clarke and Battisti theory. In the north eastern end of the head bay and the Gulf of Martaban, the geometrical configuration of the coastline, in addition to the wide continental shelf, could contribute to the amplification of both semi-diurnal and diurnal constituents. In the Malacca Strait, the amplitudes of both semi-diurnal and diurnal tides are found to increase gradually from the northern end to the 2.5°N and decreases towards southern boundary. The co-tidal and co-range charts of M_2 and S_2 tidal constituents also show the presence of two degenerate amphidromic points; one in the central part in the head bay and the other in the north eastern end of the head bay. A virtual amphidromic point for M_2 is identified in the Malacca Strait.

Keywords: semi-diurnal tides, diurnal tides, co-tidal charts, amphidromic point, Bay of Bengal.

*Corresponding author

e-mail: sindhumol123@gmail.com (B Sindhu)

unni@nio.org (A.S Unnikrishnan)

1. Introduction

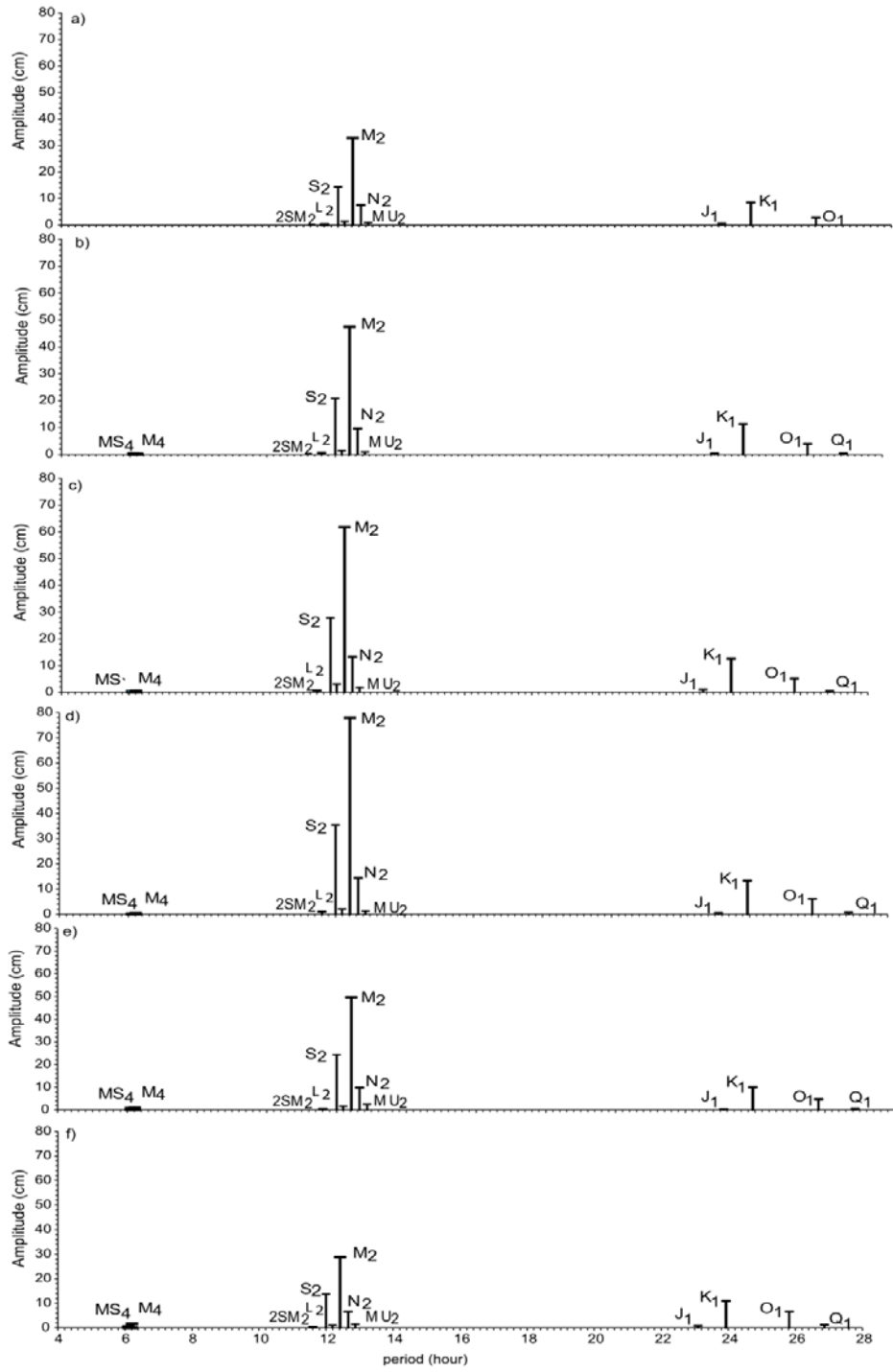
The magnitude and extent of severity of storm surges produced along a coast due to a tropical cyclone not only depends on the magnitude of meteorological forcing but also depends on the phase of tide in that location. The worst disasters occur when large surge coincide with high tide (Murty et al. 1986; Flather 1994). The real magnitude of storm surges can be predicted accurately only if the interaction between tides and surges are taken into account. Therefore, as a first step towards simulating the combined effect of tides and surges, it is useful to develop a model driven by tides alone (Jones and Davies 2005), which can be efficiently validated with locally available tide gauge records. The tidal model can, then, be modified to incorporate meteorological forcing to simulate storm surges. Following these, we developed a storm surge model to simulate the surges caused by cyclones that occurred during 1974-2000 in the Bay of Bengal and to estimate the return levels of total sea level along the east coast of India (Sindhu and Unnikrishnan, 2012). The main objective of the present paper is to describe the characteristics of tides in the Bay of Bengal using a numerical model.

Earlier, attempts to understand the characteristics of tides in the Bay of Bengal were very limited. Murty and Henry (1983) developed co-tidal charts of major tidal constituents M_2 , S_2 , K_1 , and O_1 in the Bay using a numerical model. The model was driven by tidal elevations prescribed along the southern open boundary obtained by linear interpolation of widely separated tidal observations in Sri Lanka, the Nicobar Islands and Thailand, as the information on tidal elevations in the deep regions was not available.

Fortunately, with the advent of satellite altimeter since 1992, the present global tidal models, which assimilate altimetry data, can provide reliable information on tides in oceans, except very near the coast.

The model, used in the present work, is driven by the boundary conditions obtained from the global tidal model, FES2004. A description of the model and the data used for the validation is given in Section 2. The comparison of the model results with the observations is described in Section 3. As evident from Figure 1, the major semi-diurnal and diurnal constituents that have relatively high amplitudes in the Bay are M_2 , S_2 , N_2 and K_1 , O_1 . Separate simulations were carried out for each of these major tidal constituents in order to generate co-tidal and co-range charts for the Bay of Bengal, which are presented in Section 4.

Figure 1 The amplitudes of semi-diurnal and diurnal constituents as obtained from harmonic analysis of observed sea level data available at a) Chennai, b) Visakhapatnam, c) Paradip, located along the east coast of India, d) Akyab, located along the northern coast of Myanmar, e) Sabang, and f) Sibolga located along the western coast of Indonesia. The location of these stations is shown in Figure 2 and tabulated in Table 1.



2. Data and methodology

2.1 Model Description

The model used in the present study has been described in our earlier studies (Unnikrishnan et al. 1999; Sindhu 2012; Sindhu and Unnikrishnan 2012). The model consists of a system of vertically integrated continuity equation and the equations of momentum.

$$\frac{\partial \eta}{\partial t} + \frac{\partial U}{\partial x} + \frac{\partial V}{\partial y} = 0 \quad (1)$$

$$\frac{\partial U}{\partial t} + \frac{\partial}{\partial x}(uU) + \frac{\partial}{\partial y}(vU) - fV = -gH \frac{\partial \eta}{\partial x} - \frac{C_d U \sqrt{U^2 + V^2}}{H^2} + A_H \left(\frac{\partial^2 U}{\partial x^2} + \frac{\partial^2 U}{\partial y^2} \right) \quad (2)$$

$$\frac{\partial V}{\partial t} + \frac{\partial}{\partial x}(uV) + \frac{\partial}{\partial y}(vV) + fU = -gH \frac{\partial \eta}{\partial y} - \frac{C_d V \sqrt{U^2 + V^2}}{H^2} + A_H \left(\frac{\partial^2 V}{\partial x^2} + \frac{\partial^2 V}{\partial y^2} \right) \quad (3)$$

The terms in the Equations (2) and (3) are represented in Cartesian coordinate as the time rate of change and the advective change of the depth mean current, the Coriolis force, the surface pressure gradient, the bottom stress, and horizontal diffusion term, where

t	time (s), measured relative to the commencement of simulation,
x, y	rectangular Cartesian co-ordinates (m),
$\eta(x, y, t)$	free surface elevation (m) above Mean Sea Level (MSL),
$h(x, y)$	depth of sea bed below MSL (m),
$H(x, y, t)$	total depth of the sea bed (m), i.e, $H = h + \eta$,
$u(x, y, t)$	zonal component of vertically averaged velocity (ms^{-1}) over a depth, ($h + \eta$),
$v(x, y, t)$	meridional component of the vertically averaged velocity (ms^{-1}),
$U(x, y, t)$	x - directed vertically integrated transport (m^2s^{-1}), $U = \int_{-h}^{\eta} u dz$,
$V(x, y, t)$	y - directed depth integrated transport (m^2s^{-1}), $V = \int_{-h}^{\eta} v dz$,
f	Coriolis parameter (s^{-1}), $f = 2\Omega \sin \phi$,
Ω	Earth's angular velocity of rotation (s^{-1}) $\Omega \approx 2\pi / (3600 \times 23.9333)$,
$\phi(x, y)$	latitude north ($^\circ$) ($\phi < 0$ in the Southern Hemisphere),
ρ	density of sea water, assumed constant at $\rho \approx 1027 kgm^{-3}$,
C_d	coefficient of bottom friction,
A_H	coefficient of horizontal eddy viscosity (m^2s^{-1}).

The numerical solution of the equations is obtained by discretizing the equations in space using an explicit finite difference scheme over a uniformly staggered Arakawa-C grid

and in time using leap-frog technique. The model domain covering the entire Bay of Bengal, including Andaman Sea and Malacca Strait, with south-north extension from 1.5°N to 23°N and west-east extension from 79.8°E to 103°E is shown in Figure 2. The model domain was schematized on a rectangular mesh with uniform grid spacing of 5 min (approximately 9.2 km). The Courant-Friedrichs-Lewy (CFL) criteria was used to determine the time step for a grid spacing of approximately 9.2 km and after some numerical experiments, a time step of 12 sec was chosen. The coastal boundaries were treated as impermeable by imposing zero normal flux and slip conditions at the boundaries.

There are two open boundaries on the southern end of model domain along 1.5°N latitude, separated by the land mass of Indonesia. Both the southern boundaries have east west orientation. The western open boundary is located along 79.8°E longitude with north-south orientation. The locations of the three open boundaries in the model domain are shown as dashed lines in Figure 2.

Along the open boundaries, composite tidal elevations were specified to drive the model. These were extracted from the output of the global tidal model, FES2004, as described in Lyard et al. (2006) at selected grid points, which were then linearly interpolated to obtain the tidal elevations at all grid points along the open boundaries.

The efficiency of a model to simulate tides accurately depends on the extent to which the shallow depths are represented precisely. The role and importance of the real and accurate bathymetry dataset in numerical models to reproduce the observed tidal elevations and currents have been highlighted by Jarosz et al. (2005) and Sinha et al. (2000). Therefore, the bathymetry for the domain of the model was extracted from one of our earlier works (Sindhu et al. 2007) in which improved shelf bathymetry for the Indian Ocean was prepared (http://www.nio.org/index/option/com_subcategory/task/show/title/Sea-floor%20Data/tid/2/sid/18/thid/113) by digitizing the depth contours and sounding depths less than 200 m from the hydrographic charts published by the Naval Hydrographic Office, India and merging them with the ETOPO-5 datasets through appropriate blending techniques.

The bathymetric contours for the model domain are shown in Figure 3. The maximum depth is found to be 6000 m and the minimum depth is assigned as 5 m. The variation in the width of continental shelf is clearly evident from Figure 3, with a narrow shelf (30 km) along the east coast of India which widens towards the head bay and along the southern coast of Myanmar, the width being approximately 190 km and 230 km, respectively. The entire Gulf

of Martaban is very shallow with depth less than 50 m while the depth in the Malacca Strait varies from 150 m in the northern part to less than 10 m at the southern end.

The numerical experiments were conducted for simulating composite tide as well as for individual constituents.

Figure 2 Model domain showing the 5 min (approximately 9.2 x 9.2 km) computational grid and the location of 114 stations at which the simulated tidal elevations were extracted. The stations include the 13 Standard Ports (circles) and 31 Secondary Ports (stars) at which the model derived tidal constituents are compared with the observed constituents. The names of the Standard and Secondary Ports are referred in Table 1. The dashed lines represent the two southern open boundaries along 1.5°N and the western open boundary along 79.8°E. The coastlines of the seven countries bordering the Bay of Bengal and the four maritime states along the east coast of India are highlighted with different colours.

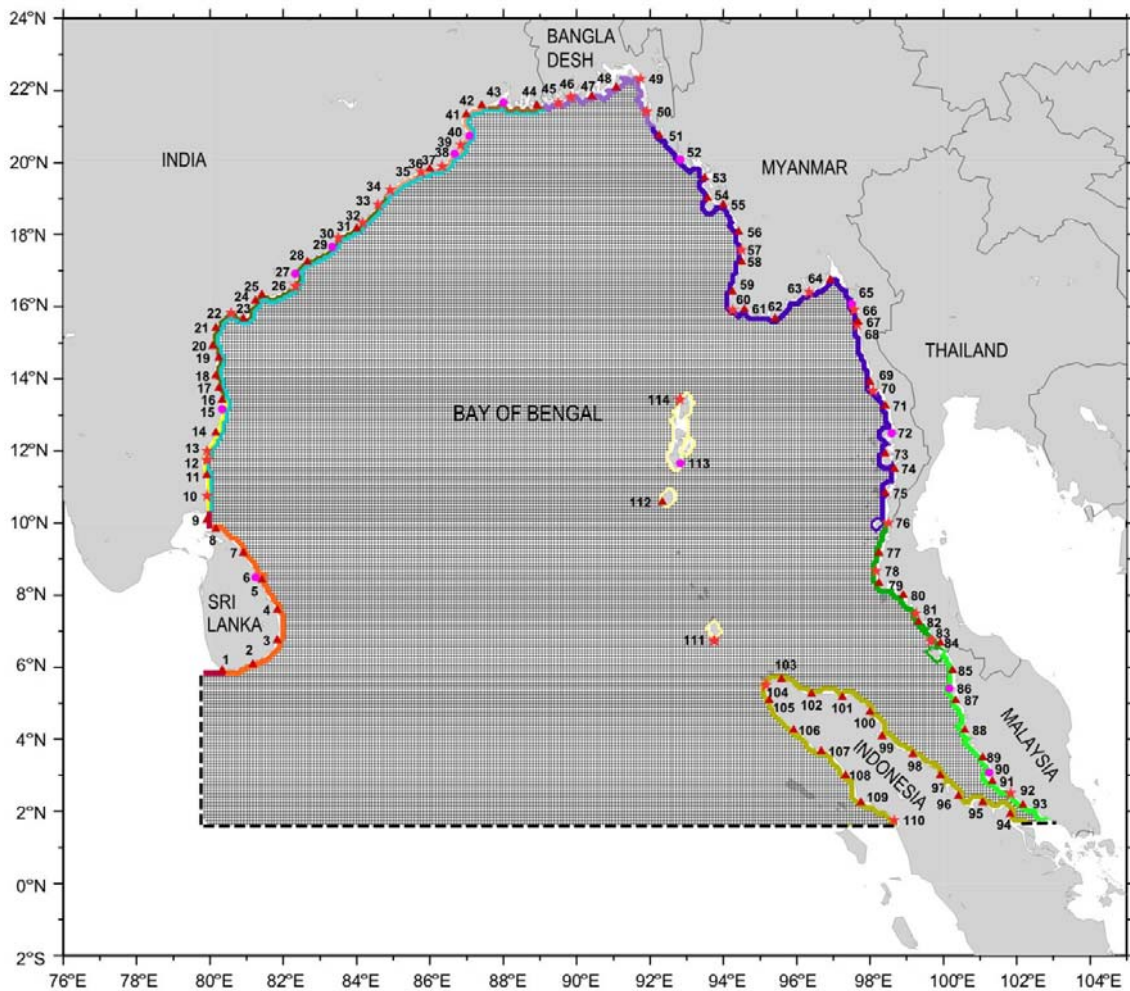
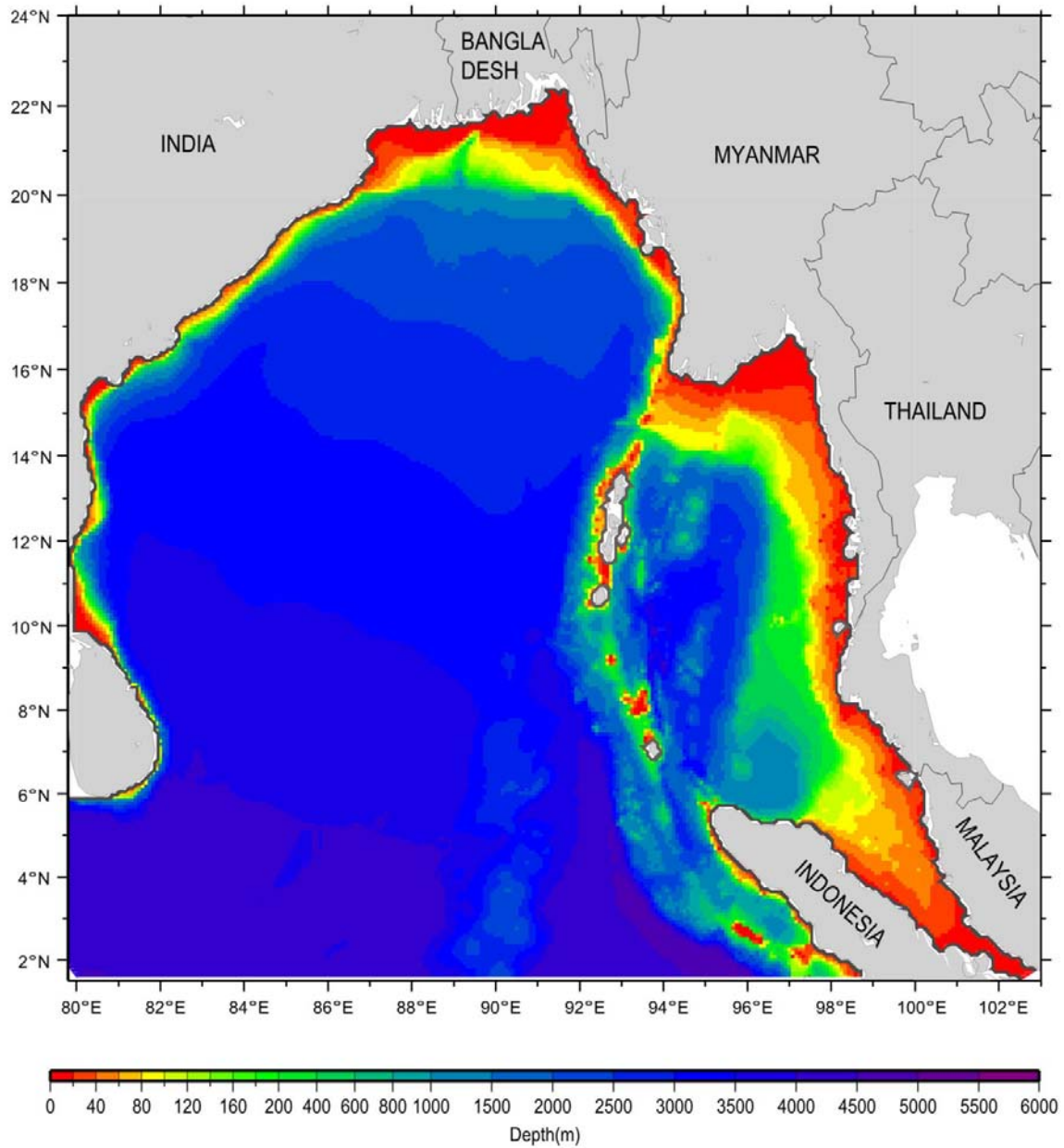


Figure 3 Bathymetry for the model domain extracted from Sindhu et al. (2007). The depths are in metres relative to MSL.



2.2 Data used for model validation

The performance of the model was assessed using the hourly data of observed sea level available from the tide gauges at Chennai, Visakhapatnam, and Paradip for the period 1974-

1988. The observed hourly time series obtained from the tide gauges at Paradip, Chennai and Visakhapatnam are relative to Chart Datum and expressed in Local Time (IST).

The model results were also compared with the tidal constituents obtained from Admiralty Tide Table (ATT), Volume 3 published by United Kingdom Hydrographic Office (UKHO 2010), which provides the amplitude and phase ‘g’ of semi-diurnal constituents M_2 , S_2 and the diurnal constituents K_1 , O_1 . Among the various ports documented in ATT, 44 ports are identified to be within the model domain in which 13 are Standard Ports and 31 are Secondary ports. The geographical locations of these ports are listed in Table 1 and displayed in Figure 2. The amplitudes and phases of the semi-diurnal constituent N_2 were obtained only at Standard and Secondary Ports along the east coast of India from the Special Publications of International Hydrographic Bureau (IHB), Monaco.

The name and location of 44 stations along with the Time Zone (relation between GMT and IST) and MSL adopted for the 13 Standard Ports covering the coast of India, Bangladesh, Myanmar, Thailand and Malaysia are listed in Table 1. Table 1 also documents the grid points (longitude and latitude) closest to the location of these 44 stations at which the simulated tidal elevations are stored.

Table 1 The name and location of 13 Standard Ports (bold) and 31 Secondary Ports as documented in Indian Tide Table and Admiralty Tide Table, respectively. The Time Zone and the height of Mean Sea Level (MSL) with respect to Chart Datum (CD) at each Port are also tabulated. The longitude and latitude of the grid points closest to location of station and the depth at that point in the model domain is also shown.

Country	St No.	Station Name	Longitude (°E) /Latitude (°N)	Time Zone (hours)	MSL (m)	Corresponding Lon(°E) /Lat(°N) in model	Depth (m)
Sri Lanka	6	TRINCOMALEE	81.217, 8.550	-5.30	0.39	81.250, 8.500	24.268
East coast of India	10	Nagapattinam	79.850, 10.767	-5.30	0.34	79.917, 10.750	11.026
	12	Cuddalore	79.783, 11.933			79.917, 11.750	16.200
	13	Pondicherry	79.833, 11.933			79.917, 12.000	18.076
	15	CHENNAI	80.300, 13.100	-5.30	0.65	80.333, 13.167	13.318
	22	Surya Lanka	80.533, 15.850			80.583, 15.833	4.932
	26	Sacramento Shoal	82.317, 16.600			82.333, 16.583	13.888
	27	KAKINADA	82.250, 16.933	-5.30	0.87	82.333, 16.917	0.293
	29	VISAKHAPATNAM	83.283, 17.683	-5.30	0.84	83.333, 17.667	23.074
	30	Bhimunipatnam	83.450, 17.900			83.500, 17.917	6.650
	32	Kalingapatnam	84.133, 18.350			84.167, 18.333	14.246
	33	Baruva	84.600, 18.867			84.583, 18.833	13.045
	34	Gopalpur	84.917, 19.267			84.917, 19.250	10.158
	35	Chilka Mouth	85.767, 19.717			85.750, 19.750	12.289

Country	St No.	Station Name	Longitude (°E) /Latitude (°N)	Time Zone (hours)	MSL (m)	Corresponding Lon(°E) /Lat(°N) in model	Depth (m)
	37	Devi River Entrance	86.367, 19.950			86.333, 19.917	17.260
	38	PARADIP	86.683, 20.267	-5.30	1.66	86.667, 20.250	5.791
head bay	39	False Point	86.783, 20.417			86.833, 20.500	9.047
	40	SHORTT ISLAND	87.067, 20.783	-5.30	1.92	87.083, 20.750	2.034
	43	SAGAR ROADS	88.050, 21.650	-5.30	3.00	88.000, 21.667	1.224
	45	Pussur River Entrance	89.467, 21.800	-6.00	1.70	89.500, 21.667	4.741
	46	Tiger Point	89.833, 21.850			89.833, 21.833	0.297
	49	Chittangong	91.833, 22.333			91.750, 22.333	2.282
	50	Cox's Bazar	91.983, 21.433			91.917, 21.417	5.561
north coast of Myanmar	52	AKYAB	92.900, 21.133	-6.30		92.833, 20.083	4.674
	57	Gwa Bay	94.567, 17.583			94.500, 17.583	15.222
	60	Bassein River Entrance	94.267, 15.867	-6.30		94.250, 15.917	3.417
Gulf of Martaban	63	Elephant Point	96.300, 16.500			93.333, 16.417	0.394
	65	AMHERST	97.567, 16.083			97.500, 16.083	5.475
	66	Double Island	97.583, 15.866			97.583, 15.917	10.304
	68	Bentinck Sound	97.683, 15.533			97.667, 15.500	-8.595
south coast of Myanmar	70	Sinbyubyin	98.250, 13.850			98.083, 13.667	-5.13
	72	MERGUI	98.600, 12.433	-6.30	2.79	98.583, 12.500	1.545
	76	Pulau Besin	98.483, 9.983			98.500, 10.000	1.183
west coast of Thailand	78	Klong Thung Maphrao	98.250, 8.600			98.167, 8.667	13.134
	81	Ko Ha Hyai	98.900, 7.467			99.250, 7.500	4.719
	83	Pulau Lela	99.700, 6.333			99.667, 6.750	7.285
Malacca Strait	86	PINANG	100.35, 5.417	-8.00	1.69	100.167, 5.417	1.264
	90	PELABUHAN KLANG	101.35, 3.033	-8.00	3.21	101.250, 3.083	10.214
	92	Port Dickson	101.783, 2.517	-8.00	1.50	101.833, 2.500	2.254
west coast of Indonesia	104	Sabang	95.333, 5.833			95.167, 5.500	20.756
	110	Sibolga	98.767, 1.750			98.667, 1.750	13.080
Andaman Islands	111	Galathea Bay	93.850, 6.783			93.750, 6.750	166.000
	113	PORT BLAIR	92.767, 11.683	-5.30	1.21	92.833, 11.667	141.770
	114	Temple Sound	92.850, 13.433			92.833, 13.417	3.855

3. Comparison with observations

The simulation of tides in the Bay of Bengal was carried out for a period of 3 months. Therefore, the tidal elevations were extracted from the FES2004 for a period of 103 days from June 20, 1981 to September 30, 1981 and prescribed along the open boundaries. Though it was experimentally evaluated that the model required 48 hours to spin-up and reach a

stable state, the model output was, however, stored from 11th day onwards. The investigation carried out by Hall and Davies (2005) implied that the accuracy of the major tidal constituents M_2 , S_2 , N_2 , K_1 and O_1 derived through harmonic analysis of short span data can be improved if the composite tidal elevations are generated from a combined effect of all constituents which includes the higher harmonics and shallow water constituents arising from non-linear interactions and the data are stored every 10 minutes. Therefore the simulated composite tidal elevations were stored at every 10 minutes for a period of 92 days at 114 grid points along the coast covering almost the entire model domain (Figure 2). The 114 stations included the 44 check stations, tabulated in Table 1, representing the locations of the Standard/Secondary Ports at which model output was compared with the observed data.

The model was calibrated through fine-tuning of friction coefficient, C_d and eddy viscosity, A_H in order to achieve maximum agreement between the simulated and observed tidal elevations. A detailed analysis of the model results obtained from a series of simulations with friction coefficient ranging from 0.001 to 0.003 suggested an improvement in the model results at shallow coastal areas with increasing C_d values while the tidal elevations in deeper waters ('h' greater than 500 m) appeared to be insensitive to friction coefficient. Therefore, following values were used for C_d :

$$C_d = 0.0025 \text{ for } h \leq 100,$$

$$C_d = 0.002 \text{ for } 100 < h \leq 500,$$

$$C_d = 0.0015 \text{ for } h > 500.$$

In order to test the sensitivity of tidal model to horizontal eddy viscosity, A_H , several experiments were carried out for uniform value of A_H ranging from 1000 to 2000 m^2/sec . Though the simulated tidal elevations were not sensitive to the changes in A_H , relatively better agreement was achieved between observed and simulated elevations for $A_H = 1500 m^2/sec$.

The validation of tidal model was carried out in two different ways:

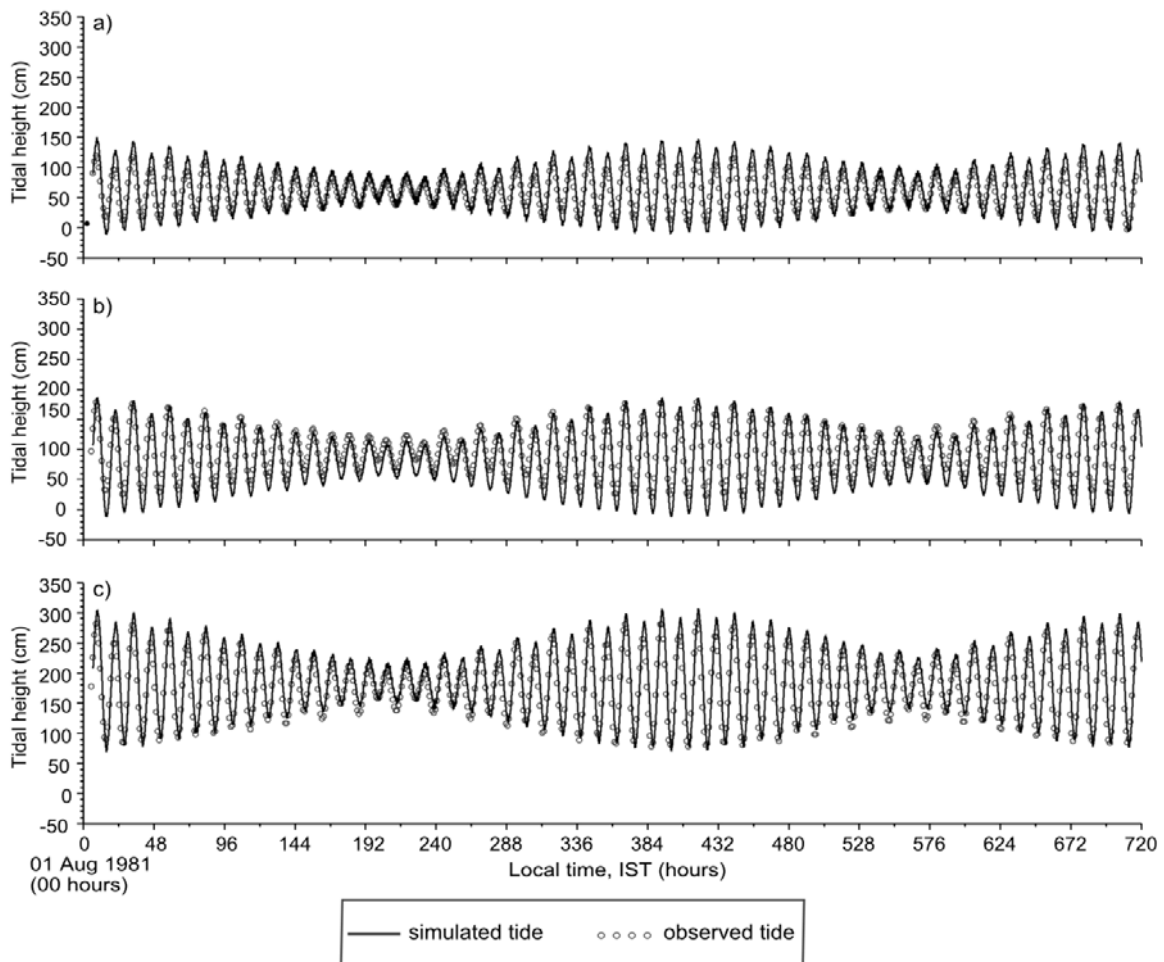
- Comparison of simulated composite tidal elevations at Chennai, Visakhapatnam and Paradip with hourly tide gauge data.
- Comparison of the model derived amplitudes and phases of the major tidal constituents at 44 stations with those documented in ATT.

3.1 Comparison with hourly tide gauge data

The simulated composite tidal elevations (after shifting the datum from MSL to CD and making necessary adjustment related to the Time Zone as per the relation listed in Table 1) were compared with the observed tide gauge data at Chennai, Visakhapatnam, and Paradip.

Figure 4 shows the time evolution of simulated and observed tidal elevations for the month of August 1981, covering a spring – neap cycle. It is evident that the mixed semi-diurnal tidal ranges and the spring-neap tidal cycles are well reproduced in the model at all the 3 stations - Chennai, Visakhapatnam and Paradip with a RMSE of 7.20, 6.74 and 7.24 cm, respectively.

Figure 4 Comparison of simulated tidal elevations (cm with respect to CD) (continuous line) with the observed hourly tidal elevations (circles) obtained from tide gauge records at a) Paradip, b) Visakhapatnam, and c) Chennai. The time 00 hours corresponds to 00 hours on August 01, 1981.



3.2 Comparison with observed amplitudes and phases of tidal constituents

The composite tidal elevation time series, obtained from model simulation, was harmonically analyzed using TASK2000 software (Bell et al. 2000), derived from the TIRA tidal analysis program (Murray 1964) to obtain the amplitude and phases G of the major semi-diurnal and diurnal constituents (referred to as 'model derived constituents' in the text). Since the span of the data analyzed was more than 90 days, the major semi-diurnal and diurnal constituents could be extracted accurately (Bell et al. 2000). The phase ' G ' of each model derived constituent at all stations was converted to include the Local Time Zone effect and obtain phase ' g ' using the Equation (4).

$$G_n = g_n + T_z \omega_n \quad (4)$$

where, T_z is the time zone defined as the shift in time at any place with respect to the Greenwich Mean Time and ω_n is the angular speed (related to period T_n as $\omega_n = 2\pi/T_n$).

Figures 5 and 6 show the amplitudes and phases of the model derived tidal constituents at 114 stations including the 44 check stations at which the observed data are available. The comparison of the amplitudes of model-derived constituent with the observed indicates that the solution fits quite well with the observations. The model derived constituents M_2 and S_2 show high variation in amplitude and the diurnal constituents K_1 and O_1 show relatively constant amplitudes along the coast of Bay of Bengal, which is in agreement with the observed amplitudes.

3.3 Statistical analysis to assess model performance

The performance of the model is demonstrated with scatter plots of model derived and observed amplitudes and phases of the tidal constituents (Figures 7 and 8, respectively). It is seen that the major semi-diurnal constituents M_2 and S_2 are simulated accurately and except for some outliers, the model derived and observed M_2 and S_2 amplitudes agree favourably with a correlation coefficient of 0.99 and 0.98, respectively. The model derived M_2 amplitudes show some discrepancies at Sagar Roads, Sabang, Galathea Bay and KoHoKya while S_2 amplitudes stand out as outliers at Sabang and Galathea Bay. However, at nearby locations of these stations, the model-derived amplitudes are found to be close to the observed amplitude suggesting the presence of some local phenomenon that the model cannot resolve. The amplitudes of diurnal constituent O_1 , being relatively lower than the semi-diurnal constituents, show larger scatter. The scatter plot for the phases of the tidal constituents

indicates good agreement between the model derived and observed phases of all constituents (correlation coefficient close to 0.99) except for O_1 which show low correlation of 0.92.

The accuracy of the model results is quantified by estimating mean error (ME) and root mean square error (RMSE) as shown in Equations (5) and (6) respectively for amplitudes and phases of each of the model derived constituents (Robertson et al. 1998).

$$ME_i = \frac{1}{N} \sum_N e_i \quad (5)$$

$$RMSE_i = \left[\frac{1}{N} \sum_N e_i^2 \right]^{\frac{1}{2}} \quad (6)$$

where \bar{e}_i is the mean error.

In addition, the overall performance of the model is measured by computing the RMS misfit (ORM) as suggested by Matsumoto et al. (2000):

$$ORM_i = \left[\frac{1}{N} \sum_N \frac{1}{2} (A_{s,i}^2 + A_{o,i}^2 - 2A_{o,i}A_{s,i} \cos(g_{s,i} - g_{o,i})) \right]^{\frac{1}{2}} \quad (7)$$

where, $A_{s,i}, g_{s,i}$ are the model derived amplitude and phase and $A_{o,i}, g_{o,i}$ are the observed amplitude and phase, respectively of the i^{th} constituent.

At majority of stations, the amplitudes of M_2 , S_2 , K_1 and O_1 derived from the model agree to within 10, 8, 8 and 5 cm, respectively of the observed values. The model on, an average, slightly over-estimates the semi-diurnal amplitudes and under-predict the diurnal amplitude. The largest discrepancies between model results and observations occur in the prediction of M_2 amplitude, as depicted by RMSE, probably due to the outliers seen in Figure 7.

The ME computed for the phases of the tidal constituents indicate a phase lag of 9 and 12 minutes for M_2 and K_1 tide, respectively, compared to the observed phases while S_2 and O_1 tides, on an average, appear to arrive earlier by 3 and 7 min, respectively than the observed tide (Table 2). The high RMSE for the O_1 phase is assessed to be due to sudden significant change in the phase observed at Sinbyubyin station (136°) compared to the neighbouring stations (approximately 315°), which cannot be resolved by the grid resolution considered in the model. If this station is neglected, the RMSE is found to be approximately 24.8° for O_1 phase.

Figure 5 Comparison of the model derived and observed amplitudes of a) M_2 , b) S_2 , c) N_2 , d) K_1 and e) O_1 . The amplitudes of the simulated constituents extracted at 114 stations are shown as continuous line while the observed amplitudes of M_2 , S_2 , K_1 and O_1 extracted from ATT at 44 stations are indicated as circles. The observed amplitudes of N_2 tide is obtained only at stations along the east coast of India from IHB. The names of the 44 stations are tabulated in Table 1. The abscissa represents the station number assigned to the 114 stations, the locations of which are shown in Figure 2.

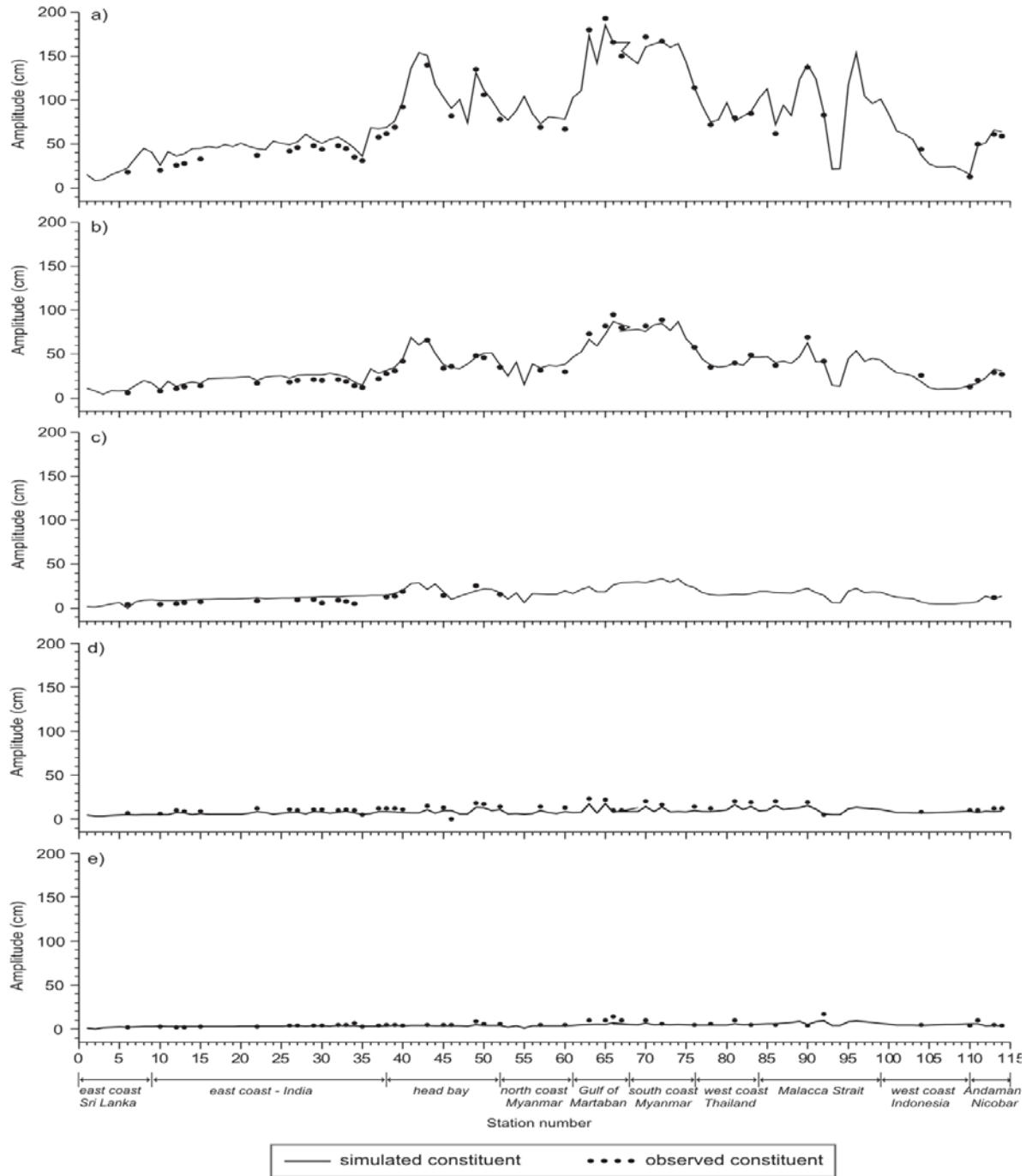


Figure 6 Same as Figure 5, but for the phases g of a) M_2 , b) S_2 , c) N_2 , d) K_1 and e) O_1 .

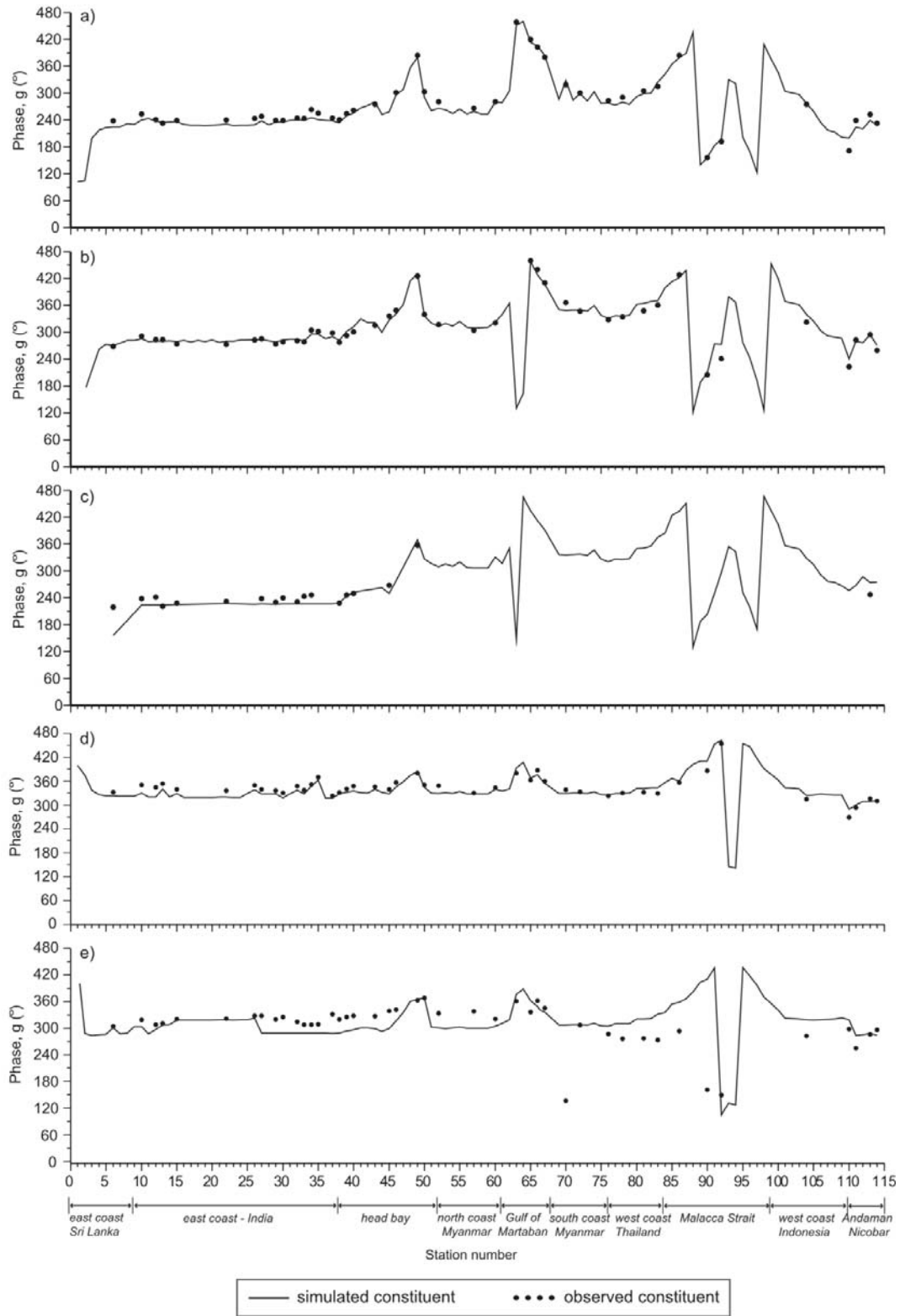


Figure 7 Scatter plots of the model derived and observed amplitudes of the tidal constituents a) M_2 , b) S_2 , c) K_1 , and d) O_1 extracted at 44 stations (locations tabulated in Table 1 and shown in Figure 1). The stations located in different regions (regions categorized as per Table 1) are marked with different symbols.

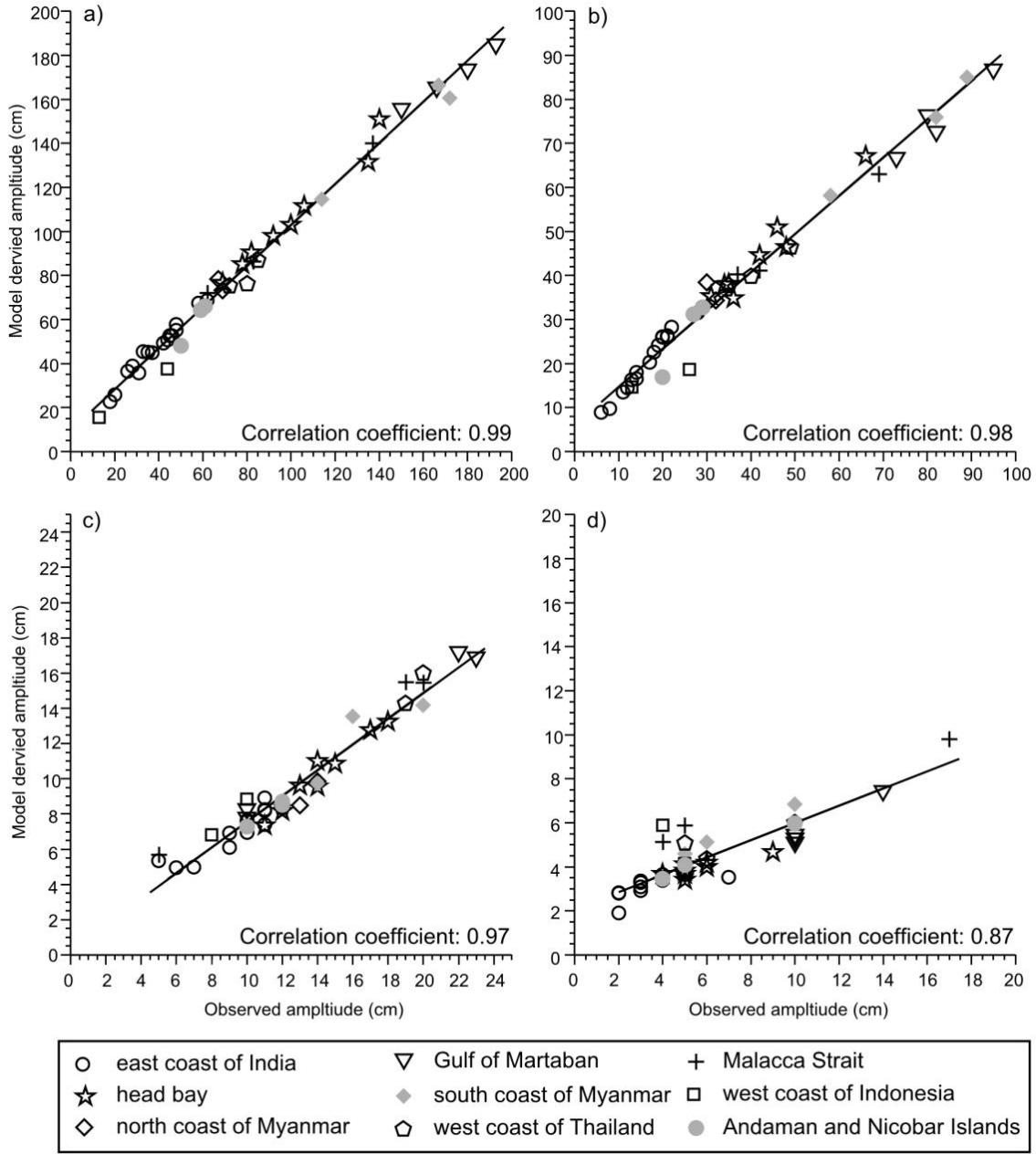


Figure 8 Same as Figure 7, but for the phases of the tidal constituents a) M_2 , b) S_2 , c) K_1 , and d) O_1 .

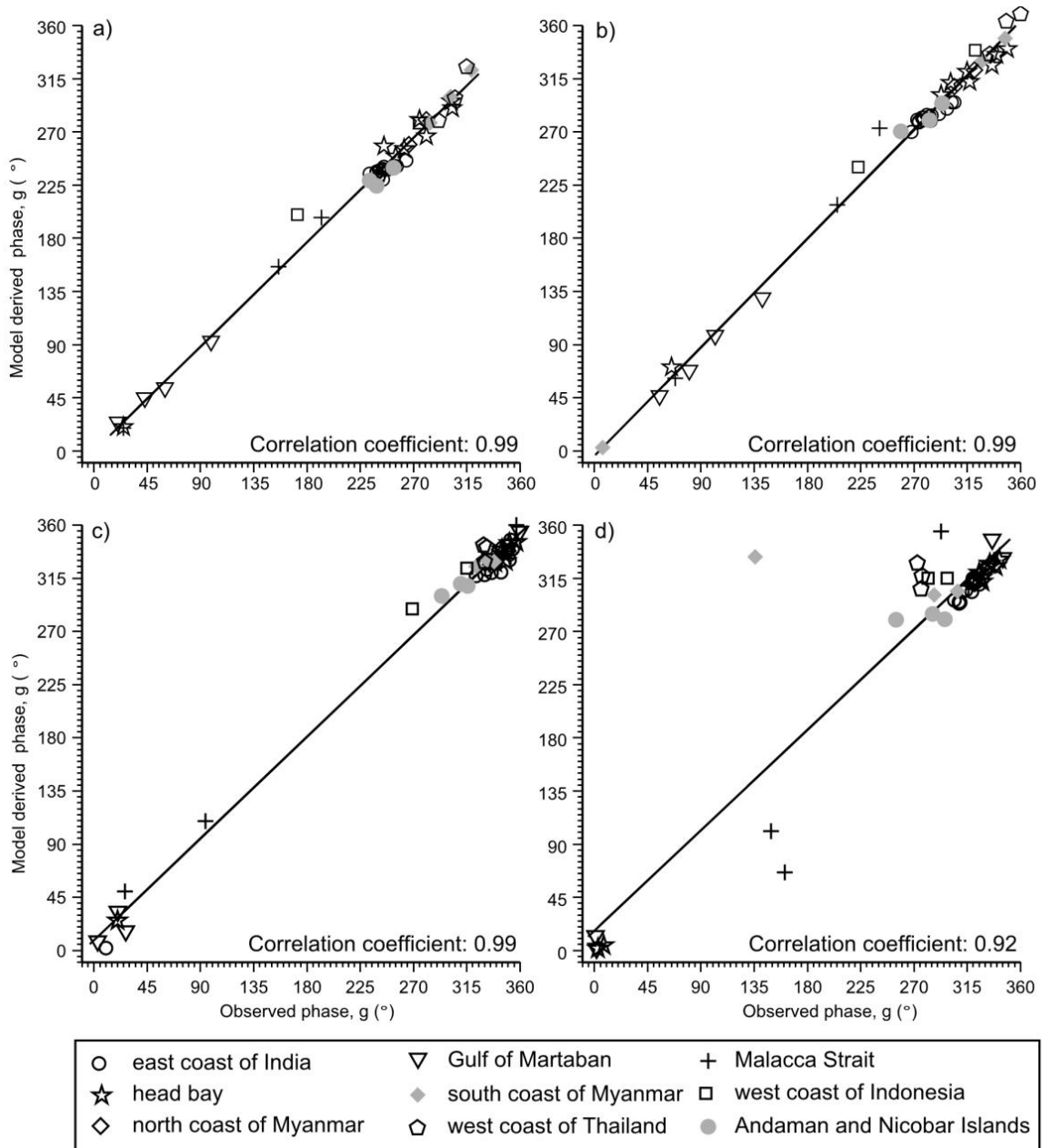


Table 2 Error statistics – Mean Error (ME) and Root Mean Square Error (RMSE) for the model derived amplitudes and phases of the major tidal constituents for the coastal stations. The Root Mean Square misfit (ORM) is also tabulated.

Constituent	ME		RMSE		ORM (cm)
	A (cm)	g (°)	A (cm)	g (°)	
M ₂	4.38	-4.18	7.04	9.43	9.16
S ₂	1.18	1.59	4.44	8.91	5.64
K ₁	-3.16	-3.64	3.45	11.06	2.89
O ₁	-1.45	1.48	2.47	38.53	3.05

On the whole, there is a reasonable agreement between the model derived and the observed amplitudes and phases of the semi-diurnal and diurnal constituents with RMSE less than 7 cm and 9.5°. It can be concluded from the RMS misfit (ORM), being less than 9 cm for all the model derived constituents, that despite of the discrepancies between the amplitudes and phases of the model derived and observed constituents at few stations, the model has the capability of reproducing the tides in the area and has sufficient fine grid to capture the near shore tidal variations.

4. Simulation of tidal constituents

The tidal elevations applied at the open boundaries of the model were modified, as described in this section, to simulate separately each of the major semi-diurnal (M₂, S₂ and N₂) and diurnal (K₁ and O₁) tidal constituents.

A time series of tidal elevation was constructed for a period of 40 days by using the amplitude and phase of M₂ tide, extracted from FES2004 dataset at selected grid points. The M₂ tidal time series was interpolated to each grid point along the open boundaries of the model. The simulated M₂ tidal elevation was stored at hourly intervals starting from the 10th day at each grid point of the model domain. The amplitudes and phases, computed from the simulated elevations of M₂ tide at each grid point of the model domain, were used to generate co-range (contour maps showing lines of equal amplitudes) and co-tidal charts (contour maps showing lines of equal phases), respectively. Similar procedure was followed for the preparation of co-charts of S₂, N₂, K₁ and O₁.

4.1 Co-range and co-tidal charts

This section describes the characteristic features of the distribution of tidal constituents in the Bay of Bengal identified from the co-range and co-tidal charts especially in the shallow regions of the Bay.

The co-range and co-tidal charts for the semi-diurnal constituents M_2 , S_2 and N_2 are presented in Figures 9, 10, and 11, respectively. The charts show a degenerate amphidromic system along the south eastern coast of Sri Lanka.

The M_2 amplitude (Figure 9a) tends to increase north and north-eastward while entering the head bay and the Gulf of Martaban. The distribution of M_2 tide in the Bay is affected by the presence of Andaman Island. In the central Bay, the M_2 tide propagates north-westward from the amphidromic point into the central bay and then attains a northward propagation in the head bay. In the Andaman Sea, tide progresses north-eastward and enters into the Gulf of Martaban while in Malacca Strait, tide propagate southward (Figure 9b).

The amplitudes of the S_2 tide (Figure 10a) are about half of those of M_2 tide and their variations are similar to those of M_2 tide. The S_2 tide propagates northward from the amphidromic point in the central Bay while in the Andaman Sea and Malacca Strait, similar to the M_2 tide, S_2 tide propagates north-eastward and southward, respectively (Figure 10b).

The amplitude of N_2 (Figure 11a) is low compared to the amplitudes of M_2 and S_2 . Though variations in N_2 amplitude in the central bay are less, local maxima occur in the head bay and in the Gulf of Martaban.

The co-range and co-tidal charts for K_1 (Figures 12a and b) depict only small variations in the amplitude and phase across the Bay. The amphidromic system identified from the co-range and co-tidal charts of the semi-diurnal tides along the south eastern coast of Sri Lanka is found to be located along the open boundary for K_1 tide. The propagation of the K_1 tide, similar to M_2 , is towards north-west and south-east in the central bay and Malacca Strait, respectively. The K_1 amplitude is found to be highest in the Malacca Strait unlike the semi-diurnal tides (M_2 , S_2 and N_2), which have highest amplitudes in the Gulf of Martaban. These localized features are described in detail in the next section.

The co-range chart (Figure 13a) of O_1 show a gradual increase in amplitude towards the head bay, but the amplitudes are very small, the maximum amplitude being 10 cm in the Malacca Strait. The degenerate amphidromic system in the O_1 chart is located at the southern tip of Sri Lanka, around which tide progresses in the counter-clockwise direction. The O_1 tide propagates northward (Figure 13b) in the central bay while in the Andaman Sea and inside

the Malacca Strait, the propagation of the O_1 tide is similar to that of K_1 with lower amplitudes.

Figure 9 Distribution of amplitudes and phases of M_2 tide in the Bay of Bengal simulated using the tidal model showing a) co-range lines and b) co-tidal lines. Amplitudes are given in centimetres and phase 'G' is given in degrees. The area marked as Detail 1, Detail 2 and Detail 3 are shown in Figure 15, Figure 16, and Figure 17, respectively.

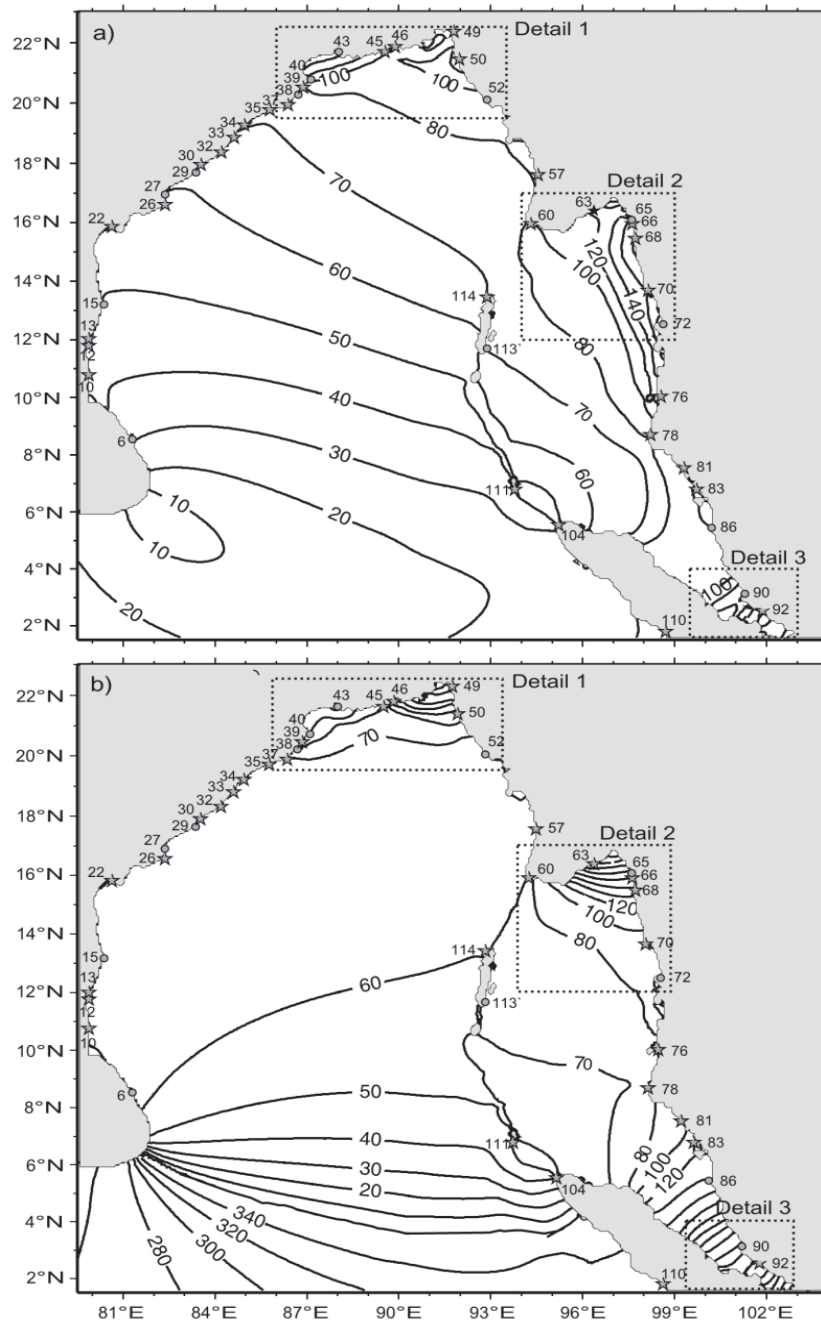


Figure 10 Same as Figure 9, but for S_2 tide.

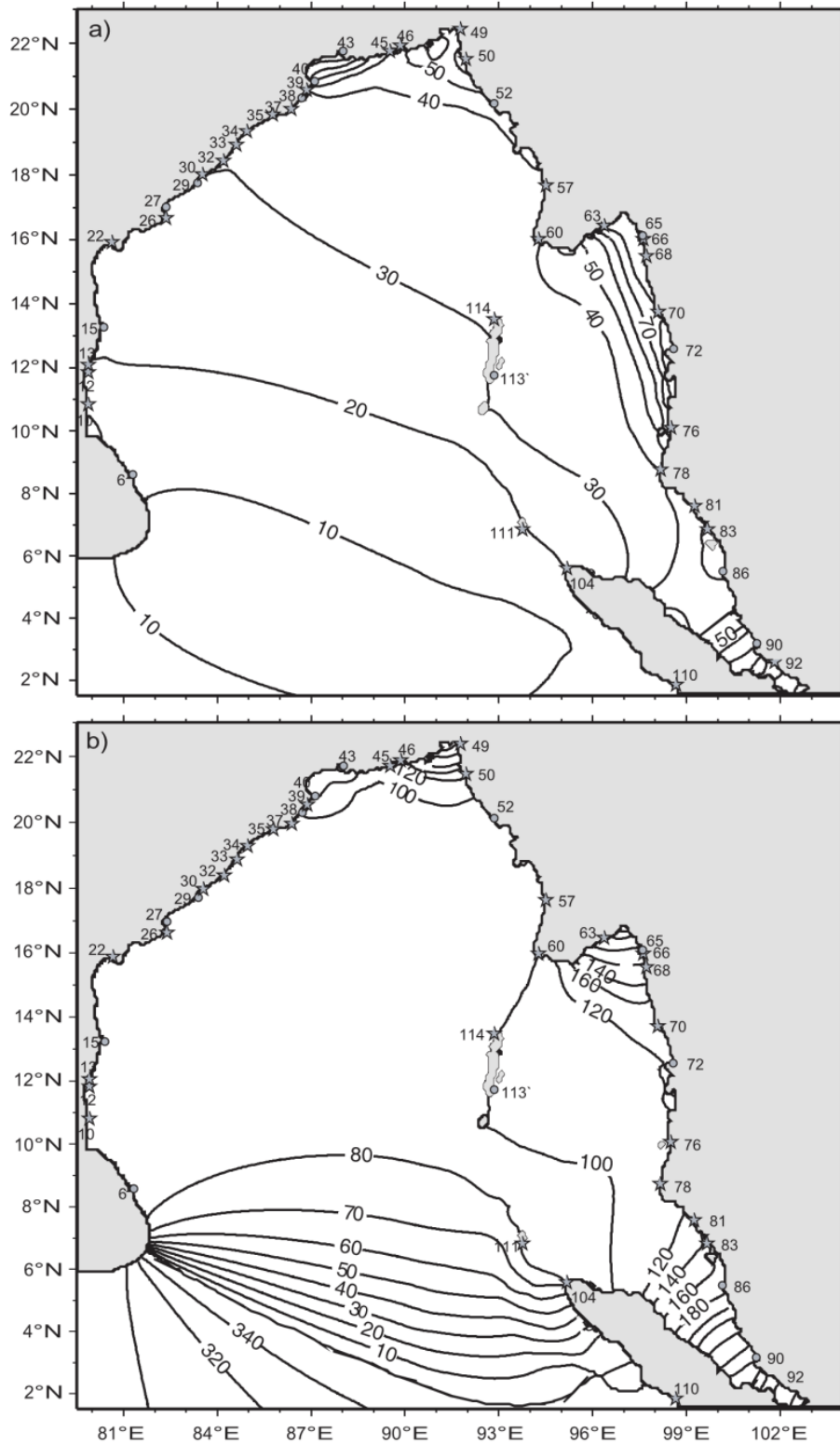


Figure 11 Same as Figure 9, but for N_2 tide.

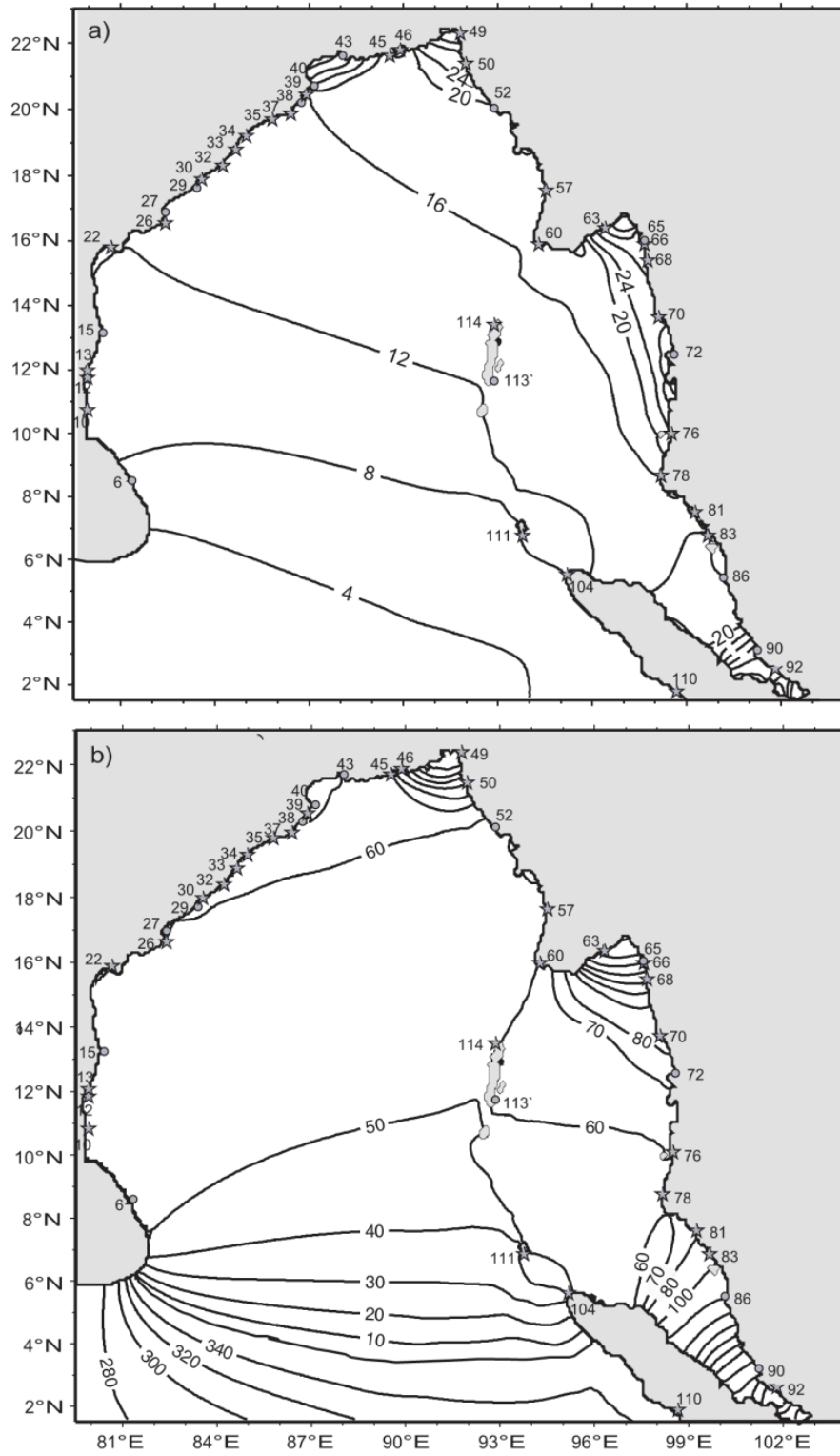


Figure 12 Same as Figure 9, but for K_1 tide. The area marked as Detail 3 is shown in Figure 17.

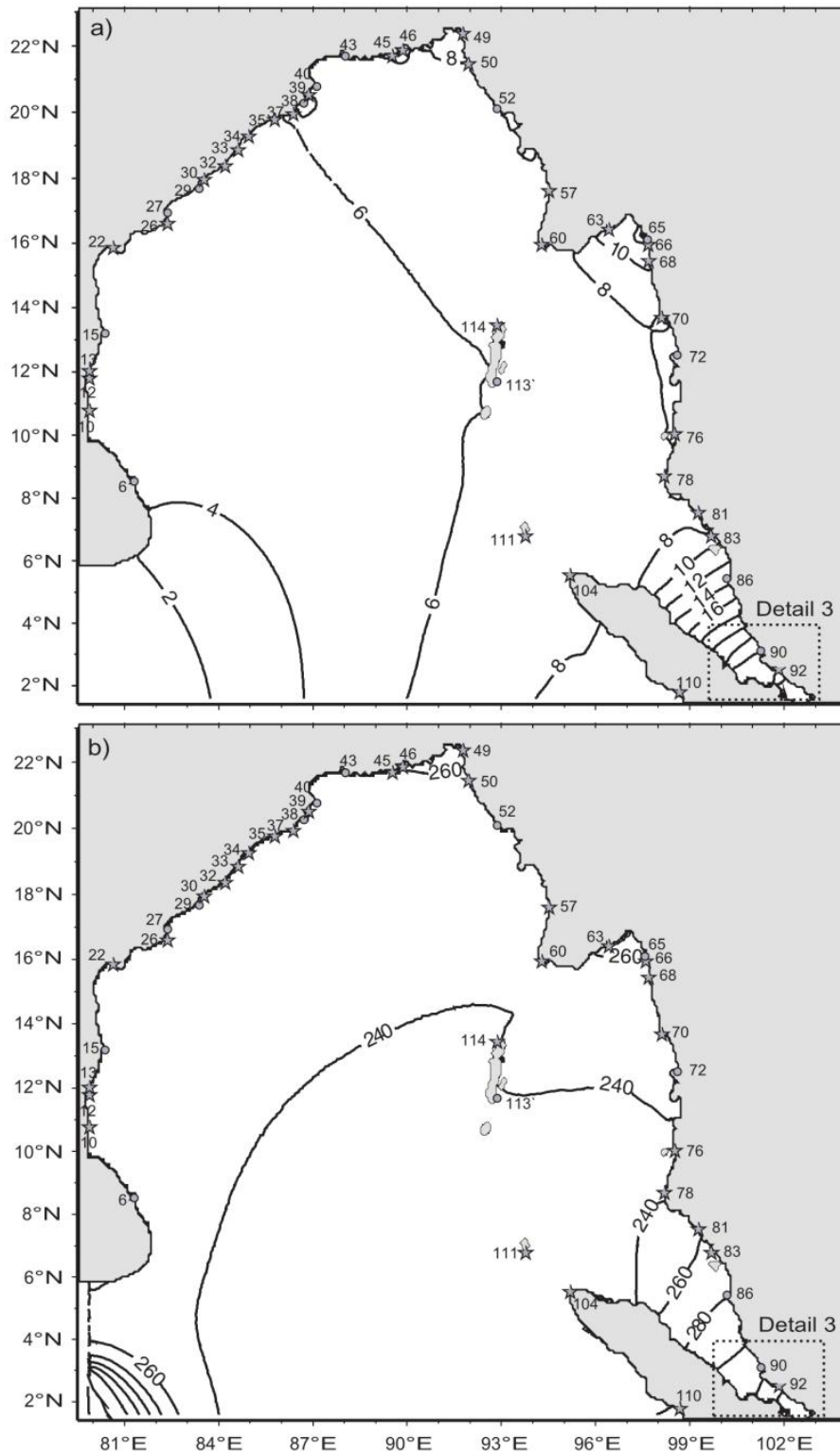
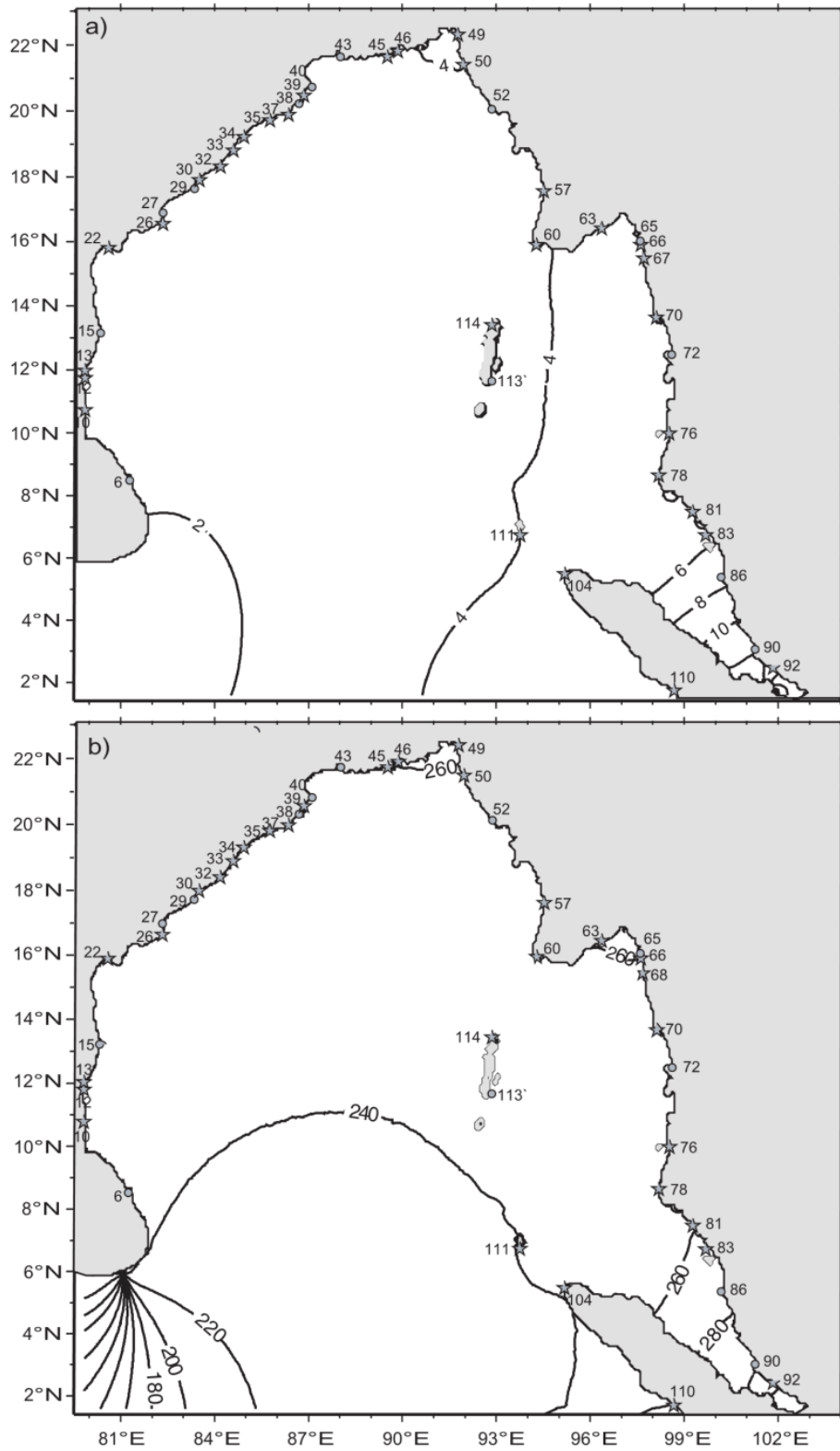


Figure 13 Same as Figure 9, but for O_1 tide.



4.2 Characteristic features

Some characteristic features are observed in the distribution of the amplitudes and phases of tidal constituents in the shallow regions of Bay of Bengal such as the head bay, Gulf of Martaban and Malacca Strait. For semi-diurnal constituents, the detailed view of the co-tidal and co-range charts in these regions is shown in Figures 15 to 17 and for diurnal constituent, the detailed view is shown only for the Malacca Strait in Figure 17.

Head Bay

The amplitudes of the semi-diurnal tides are found to be doubled in the head bay. The essential feature that could significantly contribute to the increase in the amplitudes of semi-diurnal tides in the head bay is its wide continental shelf as analyzed in the below section.

The effect of continental shelf is studied using the theory formulated by Clarke and Battisti (1981), referred to as 'CB theory' in the text. They showed that semi-diurnal tides amplify on wide shelves in non-polar latitudes while the diurnal tides do not. They related the amplification of semi-diurnal tides to the proximity between shelf width and a parameter called shelf scale parameter (defined as $SP = \frac{g\alpha}{\omega^2 - f^2}$, where α is the bottom slope, f is the Coriolis parameter and ω is the angular frequency of the tidal constituent, $\omega = 2\pi/T$, T being the constituent period).

Murty and Henry (1983) also applied the CB theory at some stations in the head bay to study the effect of continental shelf width in the head bay. But, in the present study, we applied the theory to other regions along the western and eastern coasts of the Bay. We estimated the amplification factor (AF, the ratio of tidal amplitude at coastal station to that at the shelf break) and the shelf scale parameter (SP) for M_2 , S_2 , N_2 and K_1 in order to investigate the effect of continental shelf width. Though SP and AF were extracted for all stations shown in Figure 2, except for the stations located far inside the head bay, Gulf of Martaban and Malacca Strait, Table 3 documents the values only for Standard and Secondary Ports. Figure 14 shows the impact of the continental shelf width on the variability of AF of M_2 , S_2 , N_2 and K_1 .

Amplification of semi-diurnal tides is not observed at stations along the east coast of India; where the continental shelf is narrow (width less than 100 km). But in the head bay, continental shelf widens (approximately 200 km) and therefore semi-diurnal tides amplify in the region. For instance, the M_2 , S_2 and N_2 tides attain an AF of 1.9, 2.5 and 1.9, respectively at Sagar Roads (Table 3), and an AF of 1.8, 2.3, and 1.7, respectively at Chandipur, which are

located on western part of head bay. The continental shelf at Sagar Roads and Chandipur is as wide as 195 and 160 km, respectively which are relatively closer to the value of SP as seen from Table 3. The diurnal tide K_1 amplifies only marginally in the western part of the head bay ($AF=1.1$ at Sagar Roads). This is in agreement with CB theory. However at the locations of Pussur River and Tiger Point, the amplitudes of semi-diurnal tides are not relatively high (for M_2 , $AF = 1.2$ at both stations), which could be due to relatively narrow shelf (approximately 100 km), as seen from Table 3.

Table 3 The shelf scale parameter (SP) and the amplification factor (AF - ratio of amplitude at the coastal station to that at the edge of the continental shelf) estimated for the tidal constituents M_2 , S_2 , N_2 and K_1 at stations corresponding to the Standard and Secondary Ports. The shelf width estimated at each of the stations, excluding the stations located far inside the head bay, Gulf of Martaban and Malacca Strait, is also listed.

St No	Station Name	Shelf width	M_2		S_2		N_2		K_1	
			SP	AF	SP	AF	SP	AF	SP	AF
6	Trincomalee	32	1565	1.04	1458	1.04	1627	1.01	6222	1.04
10	Nagapattinam	84	1346	1.03	1253	1.03	1400	1.01	5584	1.03
11	Porto Nova	29	1500	0.99	1400	0.98	1500	0.99	6000	0.99
12	Cudallore	57	1394	1.00	1298	1.00	1451	1.00	5925	1.00
13	Pondicherry	71	1473	1.00	1371	1.00	1533	1.00	6300	1.00
15	Chennai	32	1830	1.01	1701	1.01	1905	1.00	8086	1.00
16	Pulicat	30	2470	1.01	2300	1.01	2576	1.00	11020	1.00
18	Gudur	40	2730	1.01	2539	1.03	2845	1.00	12432	1.00
19	Nellore	20	2000	1.01	585	1.02	5900	1.00	26221	1.00
20	Kavali	40	2810	1.01	2610	0.93	2928	1.00	13168	0.99
22	Surya Lanka	37	450	1.13	418	1.14	1238	1.07	2186	1.01
24	Machilipatnam	100	1192	1.02	1106	1.02	1242	1.03	5871	0.98
26	Sacromental	30	2000	0.99	2000	0.99	652	1.00	20591	0.99
27	Kakinad	50	1813	1.02	1681	1.02	1890	1.00	9231	1.02
29	Visakhapatnam	49	1153	1.00	1069	1.00	1203	1.00	6093	1.00
30	Bhimunipatnam	58	1313	1.01	1216	1.01	1370	1.00	7027	1.01
32	Kalingaptnam	44	1325	1.00	1227	1.00	1382	1.00	7253	0.99
33	Baruva	55	1046	1.01	969	1.01	1092	1.00	5896	1.00
34	Gopalpur	83	1271	1.01	1176	1.01	1327	1.00	7345	1.00
35	Chilka Mouth	92	1049	0.99	971	0.99	1096	0.99	6267	1.00
36	Puri	85	1517	0.99	1403	0.99	1584	0.99	9113	0.99
37	Devi River	34	1887	0.99	1745	0.99	1971	0.98	11398	1.00
38	Paradip	41	569	0.93	526	0.90	594	0.88	3516	0.90
39	False Point	65	446	1.06	412	1.09	466	1.08	2809	1.01
40	Shortt Island	104	445	1.21	411	1.31	465	1.28	2858	1.05

St No	Station Name	Shelf width	M ₂		S ₂		N ₂		K ₁	
			SP	AF	SP	AF	SP	AF	SP	AF
41	Chandipur	160	840	1.78	776	2.33	878	1.72	5658	1.07
43	Sagar Roads	195	614	1.93	567	2.53	642	1.88	4257	1.13
45	Pussur River	100	677	1.25	625	1.27	708	1.04	4690	0.93
46	Tiger Point	110	657	1.21	606	1.28	687	0.99	4619	0.94
49	Chittagong	-	254	1.54	235	1.65	-	1.89	-	1.57
50	Cox Bazaar	-	232	1.32	214	1.70	-	2.00	-	1.19
52	Akyab	81	434	1.11	401	1.13	453	1.09	2651	0.99
57	Gya bay	56	2000	1.02	2000	1.02	2403	1.00	12117	1.00
60	Basien River	185	796	1.08	739	1.07	581	1.12	3880	1.10
63	Elephant	-	-	1.95	-	2.13	-	2.57	-	1.45
65	Amherst	-	-	2.41	-	2.71	-	2.21	-	1.64
66	Double Island	-	-	2.25	-	2.76	-	2.37	-	1.70
68	Bentick Sound	-	-	2.33	-	2.70	-	2.13	-	1.61
70	Sinbyubyin	204	509	1.76	473	1.85	530	1.38	2284	1.10
72	Mergui	220	386	2.00	359	2.25	402	1.63	1674	1.10
76	Pulua basin	145	711	1.51	662	1.56	739	1.32	2903	1.01
78	Klong	88	639	1.10	596	1.10	665	1.03	2547	1.01
81	KoHyaKya	157	303	1.34	282	1.41	315	1.12	1184	1.03
83	Pulua Lela	145	316	1.60	294	1.86	328	1.43	1222	1.24
86	Pinang	-	-	1.68	-	1.94	-	1.40	-	1.57
90	Pelabuhan Kl.	-	-	2.40	-	2.45	-	1.68	-	2.39
110	Sibolga	-	-	1.11	-	1.11	-	1.00	-	1.01

In the eastern part of the head bay, the amplification of semi-diurnal tides is relatively less (AF at Chittagong is 1.5, 1.6 and 1.9, respectively), but in this region the diurnal tide K₁ is observed to amplify equally as that of semi-diurnal tides as indicated by AF of 1.5 at Chittagong. Therefore, in addition to the wide continental shelf (as assessed from Figure 3), the geometrical configuration of the coastline in the north-eastern head bay could also be responsible for the amplification of both semi-diurnal and diurnal tides in the region.

The examination of the M₂ chart in detail (Figure 15b) revealed the presence of a degenerate amphidromic point near to Pussur Station. Another degenerate amphidromic point is identified at the north eastern end of head bay (Figures 15c).

Figure 14 The amplification factor (AF) of M_2 , S_2 , N_2 and K_1 tide plotted against the shelf width. The stations far inside the head bay, Gulf of Martaban and Malacca Strait have been excluded.

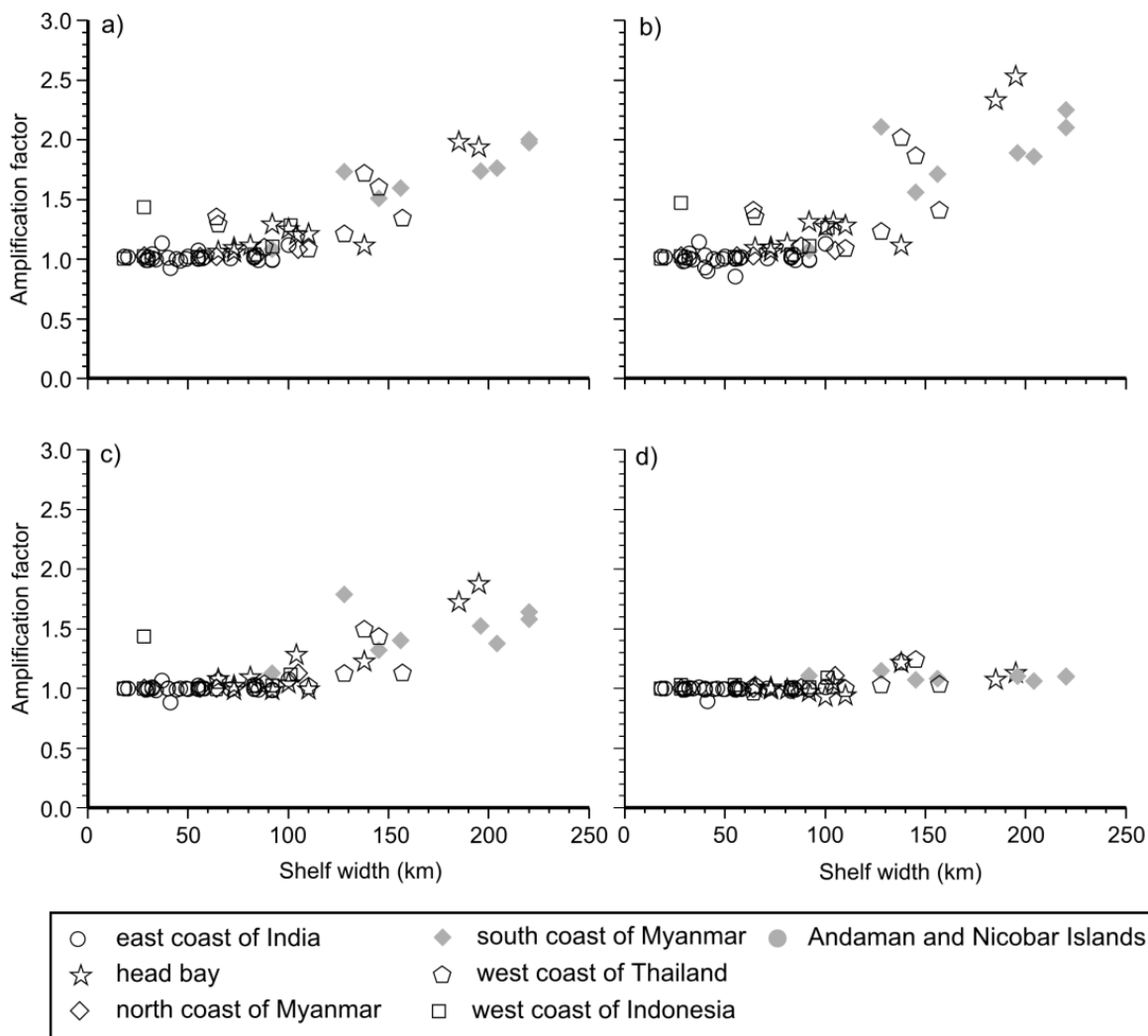
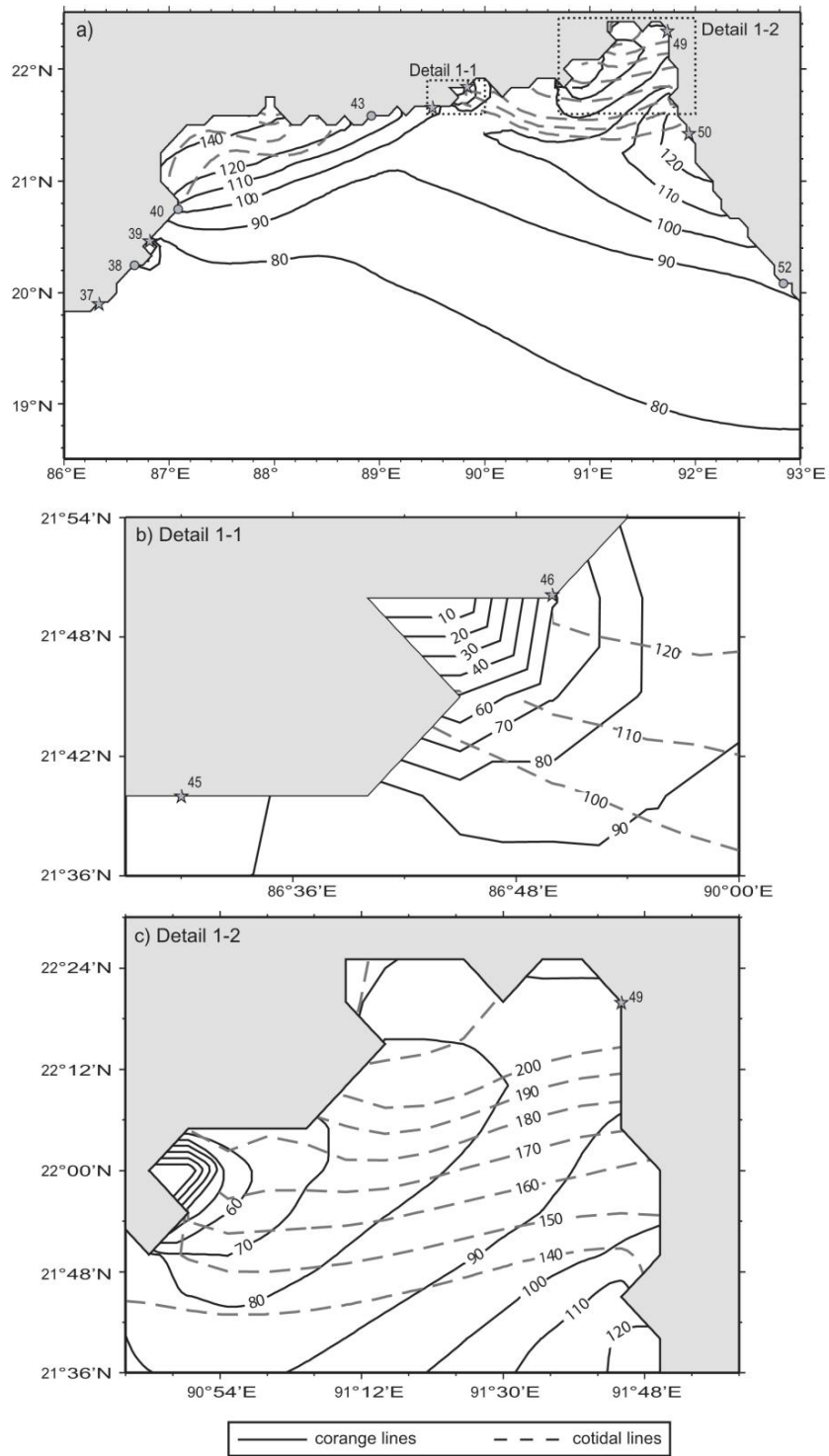


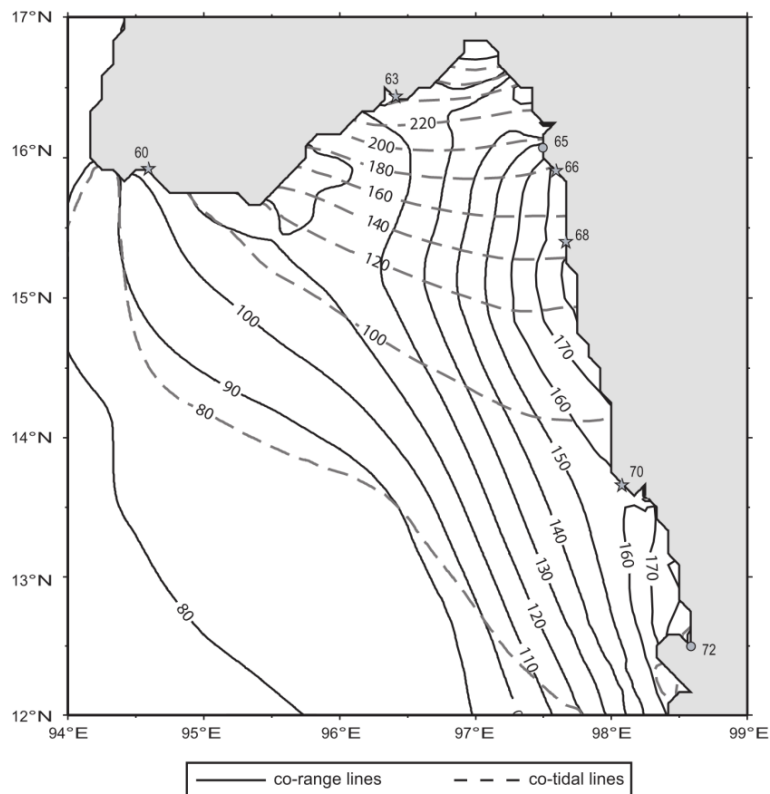
Figure 15 Detail view of co-range and co-tidal lines of M_2 tide in the a) head bay, showing the degenerate amphidromic points b) along the western coast and c) north-eastern coast of Bangladesh.



Gulf of Martaban

The co-range charts of semi-diurnal constituents (Figures 9, 10 and 11) show that along the coast of Bay of Bengal, the highest amplification of semi-diurnal tides (M_2 , S_2 , and N_2) is found in the Gulf of Martaban; the AF being 2.4, 2.8, and 2.6 (Table 3). The amplification of M_2 and S_2 are found to be higher (by 23% and 29%, respectively) along the eastern coast of Gulf of Martaban as compared to the western coast. The diurnal tide K_1 also amplifies significantly (AF=1.7) in the Gulf of Martaban. The converging effect of the funnel shaped gulf, shallow bathymetry and the wide continental shelf could contribute to the amplification, consequently producing very high tidal amplitudes in the area.

Figure 16 Detail view of M_2 tidal chart showing the co-range and co-tidal lines in the Gulf of Martaban and along the southern coast of Myanmar.



Southern part of Myanmar coast

One of the interesting features observed in the distribution of semi-diurnal co-range and co-tidal charts is the amplification of M_2 , S_2 , and N_2 along the southern coast of Myanmar, with

amplitudes increasing southward (Figure 16 for M_2) and attaining relatively higher values near Sinbyubyin (AF = 1.8, 1.9 and 1.4, respectively) and Mergui (AF = 2.0, 2.2 and 1.6, respectively) than those at Akyab and Gya Bay (AF = 1.1 and 1.0 at 2 stations, respectively for M_2 , S_2 , and N_2), which are located on the northern Myanmar coast. The coastline of Myanmar is characterized by a wide continental shelf, especially at the southern coast, where the shelf is as wide as 220 km. It is evident from Table 3 that the shelf scale parameter (SP), estimated for stations along southern Myanmar coast (Stations 68 to 72), is in close proximity to the shelf width, which signifies the amplification of semi-diurnal tides. The diurnal tide K_1 amplifies only marginally at these stations in compliance with the CB theory. Figure 14 also depicts that the variations in the amplitudes of K_1 tide is very small with the variation in shelf width along the coast of Bay of Bengal.

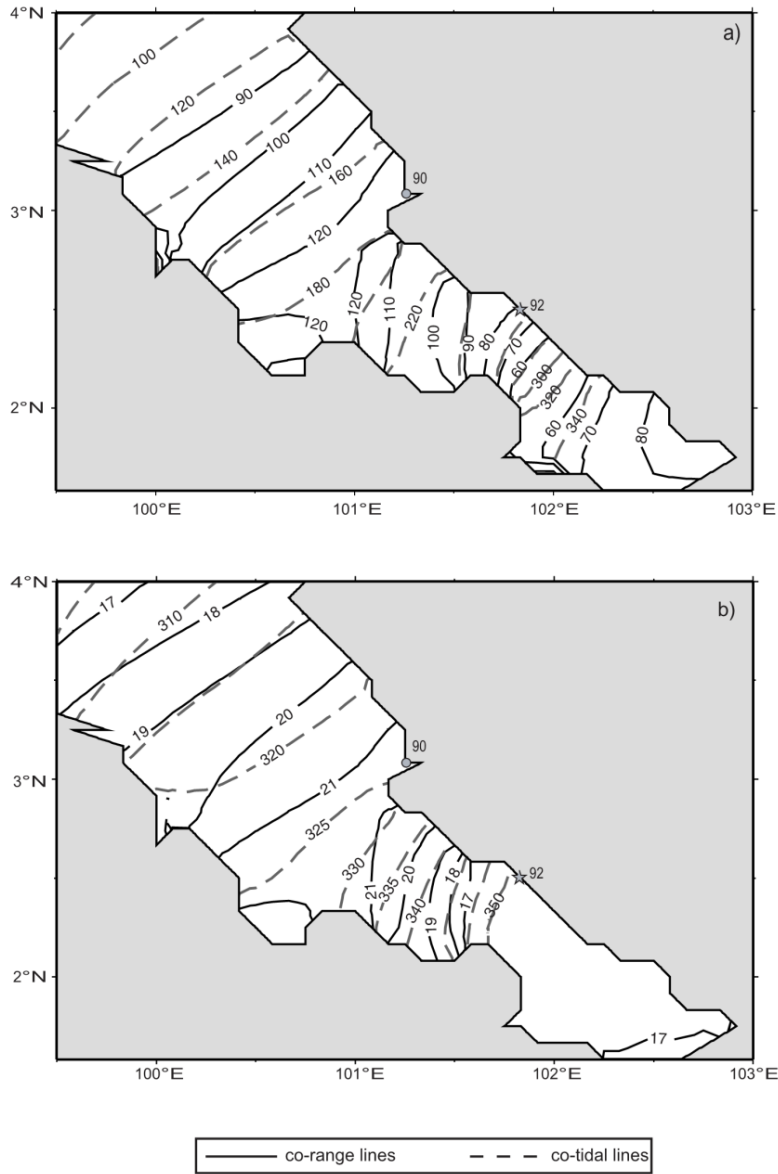
Malacca Strait

The semi-diurnal tides (M_2 , S_2 , N_2) while entering the Malacca Strait from the northern end show an increase in amplitude towards the southern region with maximum amplitude obtained at about 2.5°N (i.e. at Pelabuhan Klang, the amplitudes are as high as 130, 60 and 30 cm, respectively).

While analysing the co-range and co-tidal charts for the diurnal tide K_1 (Figure 17b), it is found that along the coast of Bay of Bengal, K_1 attains maximum amplitude (approximately 20 cm at Pelabuhan Klang) in the Malacca Strait. Even the amplitude of O_1 tide increases in the Malacca Strait (Figure 13), reaching a significant value of 12 cm at Pelabuhan Klang. It is probably the funnel shaped geometrical configuration and shallow bathymetry (depths of average 50 m) of the Malacca Strait, which are favourable for the increase in amplitudes of both semi-diurnal and diurnal tides.

However, the amplitudes of the semi-diurnal and diurnal tides are found to decrease south of 2.5°N . The amplitude of M_2 tide decreases from 2.5°N (120 cm) to 2°N (60 cm), and then again increases towards the southern open boundary. The co-range and the co-tidal pattern for M_2 tide shown in Figure 17a are similar to the distribution obtained by Rizal (2000). The decrease in the amplitude of M_2 tide is due to the presence of a virtual amphidromic point. The position of the virtual amphidromic point, as depicted from Figure 17a, could be located somewhere far inland to the north-east, which is in agreement with the findings of the Rizal (2002). The distribution of amplitudes of S_2 and N_2 and diurnal tide K_1 tide also shows signatures of virtual amphidromic point. A fine resolution tidal model for Malacca Strait is needed to confirm the presence of virtual amphidromic point.

Figure 17 Detail view of tidal chart of a) M_2 and b) K_1 showing co-range and co-tidal lines in Malacca Strait.



There is a difference in the pattern of the amphidromic points found in the eastern head bay and that in the Malacca Strait. The degenerate amphidromic point observed in the head bay is easily identifiable whereas the Malacca Strait has a purely virtual amphidromic point. This is in accordance to the conclusion of Rizal (2002) who showed that the displacement of the amphidromic systems away from the central axis decreases with the increase in the latitude and therefore the probability of occurrence of virtual amphidromes in higher latitudes

is low. It is noted that Rizal and Sundermann (1994) and Rizal (2000) simulated the semi-diurnal constituent M_2 in the Malacca Strait and explained the features exhibited by the M_2 tide in terms of virtual amphidromic point. The present work, which has the advantage of accurate open boundary conditions, is assessed to provide more accurate results.

5. Conclusions

A 2D depth averaged model was used for the simulation of tides in the Bay of Bengal. The numerical model was validated by comparing the simulated composite tides and the model derived major tidal constituents with observations at different stations covering the entire coastline.

The co-tidal and co-range charts were prepared for the constituents M_2 , S_2 , N_2 , K_1 and O_1 for the Bay of Bengal, which were analyzed in detail.

The distribution of semi-diurnal constituents (M_2 , S_2 , and N_2) shows that they amplify nearly twice in the head bay, along the southern coast of Myanmar and in the Gulf of Martaban. The diurnal constituent K_1 amplifies significantly only in the north eastern end of the head bay and in the Gulf of Martaban. The continental shelf in the head bay and along the southern coast of Myanmar is wide enough to cause significant amplification of semi-diurnal tides but do not affect the diurnal tides in agreement with the Clarke and Battisti (1981) theory. In the north eastern end of the head bay, the geometrical configuration of the coastline could also contribute to the amplification of semi-diurnal and diurnal constituents. The funnel shaped configuration of the Gulf of Martaban and the presence of wide continental shelf in this region could be the factors responsible for the highest amplification of semi-diurnal tides and relatively significant amplification of diurnal tides inside the Gulf. In the Malacca Strait, the amplitudes of both semi-diurnal and diurnal tides are found to increase from the northern end to 2.5°N , which could be due to shallow bathymetry and its funnel shaped configuration. The highest amplitudes of diurnal tides, K_1 and O_1 , are observed in the Malacca Strait. The characteristic feature observed in the Malacca Strait is the decrease in the amplitude of semi-diurnal and diurnal tides towards the southern boundary and presence of a virtual amphidromic point.

The co-tidal and co-range charts of M_2 and S_2 tidal constituents show the presence of two degenerate amphidromic points; one in the central part of head bay and the other in the north eastern end of the head bay. A virtual amphidromic point for M_2 is identified in the Malacca Strait.

The study on the propagation of tides and the distribution of amplitudes and phases of semi-diurnal and diurnal constituents in the Bay of Bengal has been scarce. Therefore, the present study focussed on the identification of characteristics features of the distribution of major tidal constituents in the Bay of Bengal, especially in the shallow regions such as head bay, Gulf of Martaban and Malacca Strait.

6. Acknowledgement

The first author thanks Council of Scientific and Industrial Research, Government of India for providing a fellowship. We thank Dr. Florent Lyard, Laboratoire d'Etude en Geophysique et Oceanographie Spatiale (LEGOS), Toulouse, France for providing the global tidal model (FES2004) results. The hourly tide gauge data were provided by the Geodetic and Research Branch, Survey of India, Dehra Dun. The present work was supported by funds from INCOIS (Indian National Centre for Ocean Information Services), Government of India. This is NIO Contribution xxxx.

References

- Bell, C., J. M. Vassie, and P. L. Woodworth. 2000. POL/PSMSL Tidal Analysis Software Kit 2000. Permanent Service for Mean Sea Level, CCMS Proudman Oceanographic Laboratory, Bidston Observatory, Birkenhead, Merseyside CH43 7RA, U.K.
- Clarke, A. J., and D. S. Battisti. 1981. The effect of continental shelves on tides. *Deep Sea Research* 28A(7):665-682.
- Flather, R. A. 1994. A storm surge prediction model for the northern Bay of Bengal with application to the cyclone disaster in April 1991. *Journal of Physical Oceanography* 24:172–190.
- Hall, P. and A. M. Davies. 2005. The influence of sampling frequency, non-linear interaction, and frictional effects upon the accuracy of the harmonic analysis of tidal simulations. *Applied Mathematical Modelling* 29:533-552.
- Jarosz, E., C. A. Blain, S. P. Murray, and M. Inoue. 2005. Barotropic tides in the Bab el Mandab Strait – numerical simulations. *Continental Shelf Research* 25:1225-1247.

- Jones, J. E., and A. M. Davies. 2005. An intercomparison between finite difference and finite element (TELEMAC) approaches to modeling west coast of Britain tides. *Ocean Dynamics* 55:178–198.
- Lyard, F. H., F. Lefevre, T. Letellier, and O. Francis. 2006. Modelling the global ocean tides: modern insights from FES2004. *Ocean Dynamics* 56:394-415.
- Matsumoto, K., T. Takanezawa, and M. Ooe. 2000. Ocean tide models developed by assimilating TOPEX/POSEIDON altimeter data into Hydrodynamical model: A global model and a regional model around Japan. *Journal of Oceanography* 56:567-581.
- Murray, M. T. 1964. A general method for the analysis of hourly heights of the tide. *International Hydrographic Review* 41(2):91-101.
- Murty, T. S., and R. F. Henry. 1983. Tides in the Bay of Bengal. *Journal of Geophysical Research* 88(C10):6069–6076.
- Murty, T. S., R. A. Flather, and R. F. Henry. 1986. The storm surge problem in the Bay of Bengal. *Progress in Oceanography* 16:195–233.
- Rizal, S. 2000. The role of non-linear terms in the shallow water equation with the application in three-dimensional tidal model of the Malacca Strait and Taylor's Problem in low geographical latitude. *Continental Shelf Research* 20:1965-1991.
- Rizal, S. 2002. Taylor's problem - influences on the spatial distribution of real and virtual amphidromes. *Continental Shelf Research* 22:2147-2158.
- Rizal, S. and J. Sündermann. 1994. On the M_2 -tide of the Malacca Strait: a numerical investigation. *Deutsche Hydrographische Zeitschrift* 46(1):61-80.
- Robertson, R., L. Padman, and G. D. Egbert. 1998. Tides in the Weddell Sea, In S. Jacobs and R. Weiss, editors, *Oceanology of the Antarctic Continental Shelf*, *Antarctic Research Series 75*, American Geophysical Union, Washington DC.
- Sindhu, B., I. Suresh, A. S. Unnikrishnan, N. V. Bhatkar, S. Neetu, and G. S. Michael. 2007. Improved bathymetric datasets for the shallow water regions in the Indian Ocean. *Journal of Earth System Sciences* 116(3):261–274.
- Sindhu, B. 2012. Numerical modelling of tides and storm surges in the Bay of Bengal. Ph.D Thesis (Submitted), Goa University, India.

Sindhu, B., and A. S. Unnikrishnan. 2012. Return period estimates of extreme sea level along the east coast of India from numerical simulations. *Natural Hazards* 61:1007-1028.

Sinha, P. C., S. K. Dube, A. K. Mitra, and T. S. Murty. 2000. A tidal flow model for the Gulf of Kachchh, India. *Marine Geodesy* 23:117-132.

UKHO. 2010. Admiralty Tide Tables, Volume 3 (2010) – Indian Ocean and South China Sea, NP 203-10. United Kingdom Hydrographic Office, Taunton.

Unnikrishnan, A. S., S. R. Shetye, and G. S. Michael. 1999. Tidal propagation in the Gulf of Khambhat, Bombay High, and surrounding areas. *Proceedings of the Indian Academy of Sciences (Earth and Planetary Sciences)* 108(3):155–177.